Zoosyst. Evol. 101 (3) 2025, 1227–1247 | DOI 10.3897/zse.101.151926

Ecological factors promote convergent evolution and ecological speciation in dwarf chameleons (*Bradypodion*)

Krystal A. Tolley[1,2], Devon C. Main[2], Keith M. Dube[2], Bettine Jansen van Vuuren[2], Jessica M. da Silva[1,2]

1 *South African National Biodiversity Institute, Kirstenbosch Research Centre, Private Bag X7, Claremont 7735, South Africa*

2 *Centre for Ecological Genomics and Wildlife Conservation, University of Johannesburg, Auckland Park, 2006, Johannesburg, South Africa*

https://zoobank.org/A22B44FA-3B22-4DA1-8031-7E73B9F01FD7

Corresponding author: Krystal A. Tolley (ktolley@uj.ac.za)

Academic editor: Justin Bernstein ♦ **Received** 3 March 2025 ♦ **Accepted** 23 May 2025 ♦ **Published** 22 July 2025

Abstract

Differing ecological conditions are considered drivers of directional selection among or between populations, resulting in ecological speciation. In particular, divergence of phenotypes in differing habitats, or convergence of phenotypes in similar habitats, can be the result of directional selection. Accordingly, species of dwarf chameleons (*Bradypodion*) that occur in structurally similar habitats tend to converge on a similar phenotype. Conversely, dwarf chameleons from contrasting habitats have been shown to diverge in phenotype. Thus, ecological speciation appears to be a mechanism for diversification in this genus. Using a combination of morphological (functional and ornamental traits) and population genetic analyses (microsatellite loci), we examined whether three closely related *Bradypodion* lineages have diverged for these dimensions. We assess whether habitats differ in structure for features related to divergence in morphological traits or whether convergence of traits corresponds to similarity in habitat structure. We find that the three taxa differ significantly at a population genetic level, but some allele sharing suggests incomplete lineage sorting or gene flow. Differences among taxa for functional traits related to gripping of branches (e.g., distal limb size [hands/feet]) can be explained by the perch diameters used by chameleons, whereas the degree of ornamentation differs among taxa in different habitats but is convergent for those in similar habitats. These outcomes are congruent with an ecological model of speciation, with taxa having diverged genetically but showing phenotypic convergence when in similar habitats and divergence when in different habitats.

Key Words

Africa, Chamaeleonidae, functional morphology, habitat structure, population genetics, reptiles

Introduction

Vicariance is considered a primary driver of diversification and speciation, whereby populations of a species become isolated due to the emergence of a barrier, with subsequent cessation of gene flow (Sanmartín and Ronquist 2004; Hoskin et al. 2005; Hoorn et al. 2010). The most obvious barriers are physical, such as geological features – rivers and lakes, islands and isthmuses, mountains and valleys, and, on a global scale, rifting of continents (e.g., Harshman et al. 2008; Hoorn et al. 2010; Rincón-Barrado et al. 2021). Vicariance events can be incorporated into a hypothesis-testing framework to assess the mode of speciation when the period of divergence is estimated and can therefore be contrasted against the date of barrier formation (e.g., Bermingham et al. 1992; Dasmahapatra et al. 2010; Tolley et al. 2013). This approach allows specific divergence scenarios to be falsified and others to be retained as plausible (see Crisp et al. 2011). Typically, the events that lead to vicariance occur over vast timescales. For this reason, speciation had long been thought to proceed only over geological timescales.

In recent decades, rapid speciation has been shown to be relatively common across the kingdoms of life

Copyright *Tolley, K.A. et al.* This is an open access article distributed under the terms of the Creative Commons Attribution License (CC BY 4.0), which permits unrestricted use, distribution, and reproduction in any medium, provided the original author and source are credited.

(Reznick et al. 2019), promoted by directional selection in response to environmental heterogeneity. However, while demonstrating vicariance-mediated speciation is relatively straightforward, evidence to support ecological processes as drivers of divergence (i.e., ecological speciation) can be less tractable, particularly in the presence of gene flow (Nosil 2008). This is because ecological barriers to gene flow are difficult to identify, and even upon their identification, they tend to be semi-permeable and dynamic, allowing for some gene flow to persist (Nosil 2008; Hendry 2009; Svensson 2012). Nevertheless, natural selection acts to distill the population of maladaptive hybridization, which is one possible explanation for how speciation might be initiated in cases where barriers to gene flow are purely ecological and porous (Butlin and Tregenza 1997; Hoskin et al. 2005). Overall, there is ample evidence that ecological processes can trigger reproductive isolation, leading to speciation through divergent or disruptive selection (Rundell and Price 2009; Schluter 2009; Öhlund et al. 2020).

Many environmental factors have been shown to contribute to the ecological diversification of populations, including macro- or microclimate (e.g., temperature, aridity), habitat type, and substrate (e.g., vegetation structure, soil type). Environmental shifts have been shown to influence species distributions (Crase et al. 2014; Lancaster et al. 2015; Musher et al. 2019). However, the emergence of novel environmental conditions could instead spatially partition populations, resulting in an environmental differential. For some species, local adaptation to the new set of environmental conditions may occur. As the barrier between the contrasting habitats becomes more robust and less permeable, gene flow would diminish, with local phenotypic forms adapted to the respective habitats becoming fixed in the corresponding diverged populations (e.g., Hewitt 1996; Ceccarelli et al. 2014; Dufresnes et al. 2020). The ecological speciation model is a viable scenario in many circumstances, but it is difficult to validate in natural populations, as the underlying evidence is essentially correlative. The model does hold, however, for controlled laboratory experiments (Rice and Hostert 1993) and is assumed to operate in nature (Losos et al. 1997, 1998; Coyne and Orr 2004; Schluter 2009). Nevertheless, replicated instances of the same phenotypic form associated with specific environments lend weight to this model, as repeated parallel evolution of similar phenotypes is less likely due to chance and more likely due to directional selection and ecological divergence. This has been demonstrated for *Anolis* lizards, both on a morphological and genetic basis (Campbell-Staton et al. 2020; Winchell et al. 2023).

Some chameleon lineages of the genus *Bradypodion* have been hypothesized to have undergone ecological speciation, even in the presence of gene flow. Specifically, taxa in novel habitats have diverged phenotypically from sister taxa that occur in the ancestral habitat (i.e., forest; Tolley et al. 2008, 2013). Conversely, where taxa occur in similar habitats, they converge on a similar phenotype regardless of ancestry (Tolley et al. 2022; Barends et al. 2024). These trends have been inferred as parallel evolution of ecomorphs that are adapted to specific vegetation substrates (e.g., Tolley et al. 2008; da Silva and Tolley 2017; Tolley et al. 2019, 2022; Barends et al. 2024). Where phenotypic divergence occurs between sister taxa, this suggests that an ecological barrier has reduced gene flow and promoted reproductive isolation, eventually resulting in genetic divergence. The new phenotype is presumably adapted to the alternative habitat state (Hopkins and Tolley 2011; da Silva and Tolley 2017; Tolley et al. 2019), pointing to ecological diversification driven by directional selection (see Schluter 2009).

The evidence for parallel evolution of phenotypes due to ecological divergence is mounting for *Bradypodion*, and each instance in which ecological diversification can be inferred is important for strengthening the case that the ecological speciation model applies. Here, we hypothesize that some lineages within the *B. ventrale* species complex have undergone ecological diversification. We propose that ecological barriers (differing habitat types) have reduced gene flow and facilitated genetic divergence, but the strength of this divergence will depend on how porous the ecological barrier is to gene flow. This, in turn, is influenced by the strength of the ecological driver (i.e., habitat) acting on phenotypes. Strong divergence of phenotypes should make the ecological barrier less porous, reducing the chances of maladaptive hybridization. Furthermore, we suggest that taxa in similar habitats should show phenotypic convergence but phenotypic divergence if in dissimilar habitats—regardless of recent shared ancestry.

We test these hypotheses for the *B. ventrale* complex, within which there are several closely related taxa (i.e., populations or species) that show reticulation of mitochondrial genes and lack of monophyly (Tolley et al. 2006). Given the mitochondrial patterns observed, we applied a suite of microsatellite loci to examine population genetic patterns at a finer scale and compared these to existing mitochondrial sequence data, supplemented with new data. This allowed us to assess the degree of admixture, given that the mitochondrial evidence suggests ecological barriers may be permeable to gene flow. To assess phenotypes, we focused on traits identified as functionally important for chameleons, for example, proximal and distal limbs and head ornamentation (see Herrel et al. 2011, 2013). These traits are considered adaptive in relation to habitat type: hand/foot and prehensile tail grip performance on branches of differing diameters has been linked to habitat structure, whereas degree of ornamentation has been associated with the mode and intensity of intraspecific communication in different habitat types (Petford et al. 2024; Barends et al. 2024). Finally, we assessed ecological differences by quantifying the widths and heights of perches available to chameleons, as well as the perches used by individual chameleons. Based on consilience of morphological, genetic, and ecological data, we propose that ecological diversification is the most likely explanation for phenotypic differences among closely related taxa, even where admixture occurs. Although geograph-

ically proximate taxa may continue to exchange genes at low levels over extended timescales, strong divergent selection in their respective environments is expected to sustain their independent evolutionary trajectories.

Materials and methods

Study group

The study included three taxa within the *Bradypodion ventrale* species complex from the Eastern Cape Province, South Africa (Fig. 1), two of which have already been described as species (see Tolley and Burger 2007). *Bradypodion ventrale* is a large, heavily ornamented species that is widespread and typically occurs in short, bushy vegetation, including thicket and Nama-Karoo. Adjacent to the range of *B. ventrale*, the vegetation consists of fynbos (a sclerophyllous heathland), which is finer in structure than the bushy vegetation typical of *B. ventrale*. Two allopatric *Bradypodion* taxa occur in fynbos, and both differ in appearance from *B. ventrale*, being smaller in body size (Barends and Tolley 2024) and having a more gracile appearance (see Tolley and Burger 2007). Of these, *B. taeniabronchum* was described in 1831 (Smith 1831) and has been recorded from four isolated populations that are separated by 20–30 km: the Elandsberg Mountains, the Tsitsikamma Mountains, and two lowland fynbos sites – Thyspunt Nature Reserve and Honeyville Nature Reserve. These populations may once have been more continuous, either historically or in modern times, but the habitat between them has been transformed by various types of agriculture and infrastructure. Thus, it is likely that the present-day isolation of populations is due to recent habitat loss. In addition, a population of *Bradypodion* occurs in the fynbos habitat on the Groot Winterhoek Mountains (hereafter referred to as *B.* "groendal," after the Groendal Nature Reserve that spans part of these mountains). This taxon has not yet been described as a species due to uncertainty regarding its relationship to *B. ventrale* and the extent to which these taxa have diversified along the species diversification continuum (sensu de Queiroz 2005). Despite the complications surrounding *B. ventrale* and *B.* "groendal," the two taxa are ecologically distinct, with *B.* "groendal" occurring at high elevation in fynbos, whereas *B. ventrale* occurs in the surrounding lowland landscape in bushy thicket vegetation (Figs 1, 2). The boundary between fynbos and bushy lowland vegetation is likely to be an ecological barrier between *B. ventrale* and the two fynbos taxa. Nevertheless, the mitochondrial haplotypes of these taxa are closely related, with some reticulation (Tolley et al. 2006), suggesting gene flow in the recent past, which may still be ongoing. Given the uncertain taxonomic status of *B.* "groendal," we refer to all the entities as 'taxa,' recognizing that two of them are formally described species and one is not. In addition, within *B. taeniabronchum*, we refer to the geographically isolated groups as 'populations.'

Sampling protocols

Chameleons were located at night with the aid of a powerful torch (Suppl. material 1: table S1). Males were identified by the presence of an external hemipenal bulge, and females by its absence. The smallest individuals with a visible hemipenal bulge were considered the cut-off size for adults, with individuals smaller than this (< 36 mm snout–vent length) classified as juveniles and excluded from the analyses. For the population genetic analyses, tissue samples (tail tips) were collected (Fig. 2) and stored in either 99% ethanol or 20% DMSO saturated with NaCl at –40 °C.

Morphology

For the morphological analyses, a total of 232 dwarf chameleons ($n_{females}$ = 111; n_{males} = 121) were measured. Chameleons were located and captured as described above and temporarily removed from their habitat overnight, kept separately in 5-L ventilated containers supplied with vegetation. Measurements were taken the next day, after which each chameleon was released at the exact point of capture (coordinates recorded by GPS and branches marked with flagging tape). Measurements were taken to the nearest 0.01 mm using digital callipers on the right side of the individual (Suppl. material 1: fig. S1): snout–vent length (SVL), tail length (TL), casque head length (CHL), head length (HL), head width (HW), head height (HH), casque head height (CHH), casque height (CH), coronoid process of mandible to snout tip (CT), lower jaw length (LJL), posterior surface of quadrate to snout tip (QT), upper arm (humerus) length (HM), forearm (radius) length (RD), thigh (femur) length (FM), shin (tibia) length (TB), width of lateral carpal bones (CAR), width of outer tarsal bones (TAR), medial hand pad plus fingers (MHF), lateral hand pad plus fingers (LHF), medial foot pad plus toes (MFT), and lateral foot pad plus toes (LFT).

All analyses were carried out using IBM SPSS Statistics v. 27. All morphometric data were $\log_{10}$-transformed to satisfy assumptions of normality and homoscedasticity. *Bradypodion* are sexually dimorphic (Hopkins and Tolley 2011; da Silva and Tolley 2013); therefore, the dataset was separated by sex for subsequent morphometric comparisons between taxa. To allow for comparisons between individuals of different sizes and to remove the effect of body size, each trait was regressed against snout–vent length (SVL), and the unstandardized residuals were saved and input into a principal components analysis (PCA). The robustness of the datasets was first examined by the Kaiser–Meyer–Olkin (KMO) test, and the contributions of each variable to overall variation were assessed by communalities greater than about 0.5 (Tabachnick and Fidell 2019). The PCA was run with varimax rotation, and principal components (PCs) with eigenvalues > 1 were extracted. The extracted PCs were then used as input for a multivariate analysis of variance

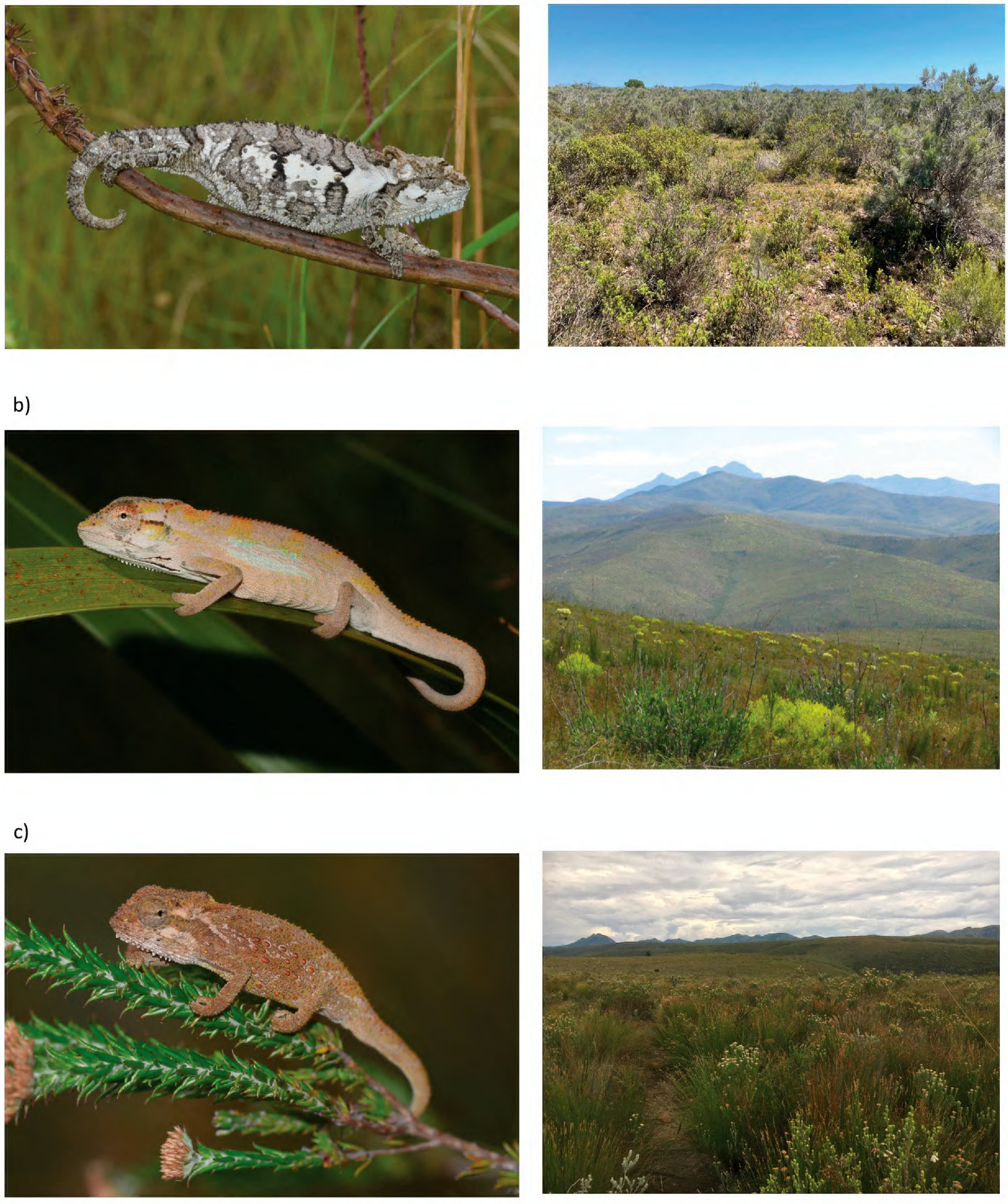

Figure 1. Chameleons of the *Bradypodion ventrale* species complex (left) and their respective habitats (right): **a.** *B. ventrale*; **b.** *B. taeniabronchum*, and **c.** *B.* "groendal."

(MANOVA) with taxon as the fixed factor. We also evaluated the probability of each individual's assignment to *B. ventrale*, *B. taeniabronchum*, or *B.* "groendal" by carrying out a discriminant function analysis (DFA) in SPSS using the regression residuals as input and taxon as the grouping variable. The DFA was run with cross-validation classification and taxon as the grouping variable.

Habitat

To assess habitat (perch) structure and use, we employed three complementary approaches. First, the width of the perch on which each chameleon was found was measured to the nearest 0.1 mm using digital calipers, and perch height was measured to the nearest 1 cm using a digi-

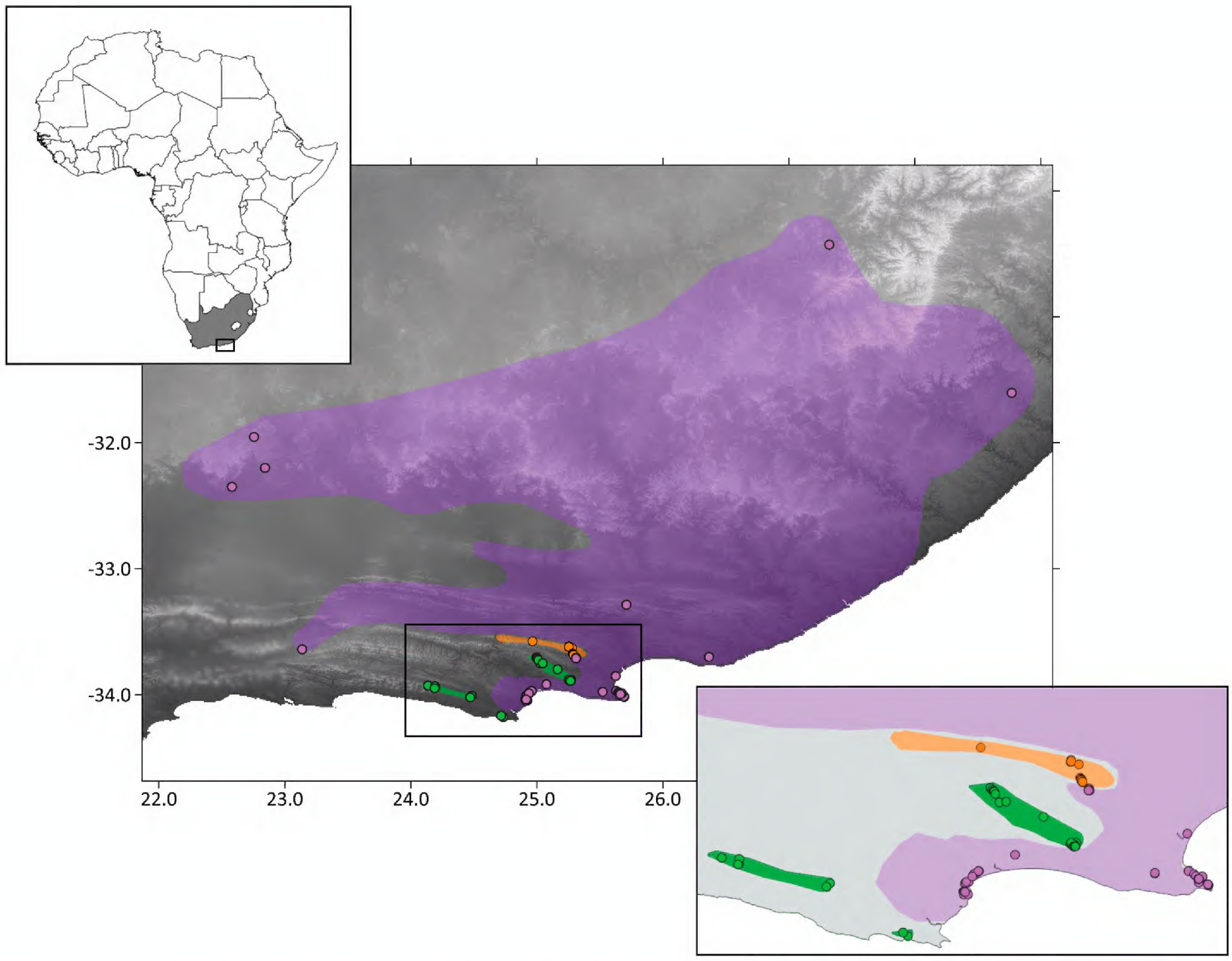

Figure 2. Sampling localities for the *Bradypodion ventrale* species complex, color-coded by taxon. Interpreted distribution maps are shown as colored polygons: *B. ventrale* (purple), *B. taeniabronchum* (green), and *B.* "groendal" (orange).

tal laser. The diameters and heights of perches used by the three taxa – *B. ventrale* (n = 142), *B. taeniabronchum* (n = 86), and *B.* "groendal" (n = 72) – were compared. Second, data on available habitat structure were collected by measuring perch diameters along transects at the same sites where chameleons were sampled. At least three 100-m transects were established per site, and perches were measured at 10-m intervals within a 1-m-wide swathe. These measurements were pooled by taxon, yielding sample sizes of 1,337 for *B. ventrale*, 3,267 for *B. taeniabronchum*, and 1,431 for *B.* "groendal." Measurements were taken approximately 10 cm below the vegetation canopy, corresponding to the height range where chameleons are most commonly observed perching (KAT and DCM, pers. obs.). Third, we compared the perches actually used by chameleons to those available in the habitat for each taxon separately to test whether perch use was random or indicated selective preference for particular perch diameters.

Prior to comparing perch diameter and height among taxa, the influence of body size on perch use was evaluated by linear regression analyses of snout-vent length (SVL) as the independent variable, conducted separately for each species. Based on these regressions (see Results), SVL was included as a covariate in analyses involving perch width but excluded for analyses involving perch height. Data suitability for parametric tests was assessed using Levene's test for homogeneity of variances. The perch width data violated the homogeneity assumption (Levene's Statistic = 26.022; $df_1 = 2$; $df_2 = 266$; $p \leq 0.001$), whereas the perch height data did not (Levene's Statistic = 1.573; $df_1 = 2$; $df_2 = 252$; $p = 0.21$). Therefore, differences among taxa in perch diameters used were assessed using a non-parametric analysis of covariance (Quade test) with SVL as the covariate. For perch height, a one-way analysis of variance (ANOVA) was applied, followed by Tukey's *post hoc* tests for pairwise comparisons.

To test for differences in available perch diameters (habitat structure) among the three taxa, a Kruskal-Wallis test was used, with pairwise comparisons conducted using Mann-Whitney U tests. Finally, to determine whether perch widths used by chameleons differed from those available in the habitat, Mann-Whitney U tests were applied separately for each taxon, comparing perch diameters used by chameleons to those measured along transects.

Population genetics

Population genetic analyses were conducted on two datasets: (1) mitochondrial ND2 sequence data, largely obtained from GenBank and supplemented by new samples filling geographic gaps, and (2) a microsatellite dataset primarily comprising new samples collected from the same localities as the mitochondrial data (Suppl. material 1: table S1). Due to depletion of original ND2 samples, it was not possible to match all individuals across datasets; thus, the datasets represent individuals from matching localities but not identical individuals. For new samples, total genomic DNA was extracted from tissue samples using a standard salt extraction protocol (Aljanabi and Martinez 1997), and DNA concentrations were standardized to 25–50 ng/µl.

The ND2 gene was amplified via polymerase chain reaction (PCR) using primers L4437 and H5934 (Macey et al. 1997a,b). The PCR protocol included an initial denaturation at 95 °C for 4 min, followed by 35 cycles of denaturation (94 °C, 45 s), annealing (55 °C, 45 s), and extension (72 °C, 1 min), with a final extension at 72 °C for 10 min. PCR products were visualized on a 1% agarose gel, and Sanger sequencing was performed by Macrogen (Amsterdam, The Netherlands) using the forward primer. Sequences were quality-checked and aligned in Geneious v11 (http://www.geneious.com). The alignment was imported into PopArt 1.7 (Leigh and Bryant 2015) to construct a median-joining haplotype network. Because this network is distance-based and lacks an explicit evolutionary model, we complemented it with a model-based maximum likelihood (ML) analysis. The ML dataset included 3–6 ND2 sequences per taxon within the focal clade, plus two individuals from each of four closely related *Bradypodion* species, including *B. atromontanum* as the outgroup (see Tolley et al. 2004). These additional sequences were downloaded from GenBank (Suppl. material 1: table S2), and all sequences were aligned in Geneious. ML analysis was conducted using RAxML (Stamatakis 2014) via the CIPRES platform (Miller et al. 2010), applying the GTR + I + G substitution model and automatic bootstrap halting. Nodes with bootstrap support > 70% were considered well supported.

Eighteen microsatellite markers specifically developed for *Bradypodion* were amplified, multiplexing up to four polymorphic primers when possible (Suppl. material 1: table S3). Fifteen markers were previously published (Feldheim et al. 2010, 2012), and three were newly developed for this study. PCR was conducted in 10 µL volumes containing approximately 30–40 ng DNA template, 2X QIAGEN Multiplex PCR Master Mix, 10× primer mix (2 µM each primer), and RNAse-free water, maintaining a 1:1 ratio of Master Mix to primer mix and DNA template, per manufacturer's instructions (QIAGEN Multiplex PCR Kit; QIAGEN, Valencia, CA, USA). Thermal cycling followed QIAGEN's microsatellite protocol: 95 °C for 15 min; 40 cycles of 94 °C for 30 s, locus-specific annealing temperature for 90 s (see Suppl. material 1: table S3), 72 °C for 60 s; and a final extension at 60 °C for 30 min. Two microliters of PCR products were visualized on ethidium bromide-stained 1.5% agarose gels with a 100 bp ladder. Successful products were genotyped at the Central Analytical Facility (CAF), Stellenbosch University, on an ABI 3500xl Prism using GeneScan 500 LIZ as an internal size standard and POP-7 polymer. Alleles were scored and binned using the microsatellite plugin in Geneious v7.1.9 (http://www.geneious.com) and exported as Excel files.

Microsatellite data were screened for genotyping errors, heterozygote deficiencies, and null alleles using MICRO-CHECKER v2.2.3 (Van Oosterhout et al. 2004). If null alleles were detected, allele and genotype frequencies would be adjusted statistically using the Brookfield 1 algorithm (Brookfield 1996) to account for expected homozygotes (e.g., Roques et al. 1999; Chapuis and Estoup 2007), with affected alleles coded as missing data. All subsequent analyses were performed on both corrected and uncorrected datasets.

Because clustering algorithms may overestimate population structure, especially in datasets characterized by isolation by distance (IBD) (Frantz et al. 2009; Schwartz and McKelvey 2009; Tucker et al. 2014), multiple algorithms were employed to identify clusters (K) of genetically related individuals, and the outputs compared. Moreover, the presence of IBD was also investigated. Together, the most likely population structure can be empirically inferred (as recommended by Guillot et al. 2008). Specifically, we used two Bayesian individual-based clustering algorithms – STRUCTURE v2.3.4 (Falush et al. 2003; Pritchard et al. 2000) and Geneland v4.9.2 (Guillot et al. 2005) – and one multivariate ordination method, discriminant analysis of principal components (DAPC) implemented in the R package 'adegenet' (Jombart et al. 2010). STRUCTURE infers genetic clusters based solely on multilocus genotypes (Pritchard et al. 2000; Falush et al. 2003), whereas Geneland incorporates spatial coordinates, which can enhance clustering support, especially with sparse sampling (Ball et al. 2010). Unlike the Bayesian approaches, DAPC makes no assumptions about population genetic models (Jombart 2008; Jombart et al. 2010). Concordant results across methods indicate robust inference of spatial genetic structure (Rutledge et al. 2010; Blair et al. 2012; Aurelle and Ledoux 2013).

For STRUCTURE and Geneland, the number of clusters (K) was tested from 1 to 10, exceeding the number of sampling sites (Suppl. material 1: table S1). STRUCTURE was run with 10 independent runs per K, using the admixture model and correlated allele frequencies, with 300,000 MCMC iterations after a burn-in of 100,000. STRUCTURE HARVESTER v0.6.94 (Earl and von Holdt 2012) was used to estimate the optimal K based on the ΔK method (Evanno et al. 2005). The 10 runs for the optimal K were processed with CLUMPP v1.1.2 (Jakobsson and Rosenberg 2007) using the Greedy algorithm (M = 2) to correct for label switching and multimodality. Results were visualized as barplots using DISTRUCT v1.1 (Rosenberg 2004).

In Geneland, analyses used the correlated allele frequency model with 10 independent runs of 500,000 MCMC iterations (thinning = 100), no filtering of null alleles, and delta coordinate set to 0 (reflecting exact spatial coordinates of individual captures, justified by the species' low vagility; da Silva and Tolley 2017). Default values were used for all other parameters. Post-processing used a burn-in of 100 iterations to generate posterior probabilities of population membership for each individual and spatial pixel (200 × 200 grid). Consistency across runs was visually confirmed. Geneland's post-processing corrects for label switching, so CLUMPP was not applied. Bar plots of cluster membership were produced with DISTRUCT.

For each program, the most reliable model and K were identified by evaluating run consistency and assessing the biological meaningfulness of inferred clusters across the landscape.

Isolation by distance within clusters and the entire dataset was tested with Mantel tests of matrix correspondence in GenAlEx 6.5 (Peakall and Smouse 2006) using 9,999 permutations. A positive correlation ($R_{xy}>0$) between genetic and geographic distances indicated IBD.

Population structure from DAPC was further assessed by an analysis of molecular variance (AMOVA) and pairwise R_{ST} values, calculated in ARLEQUIN 3.5.1.2 (Excoffier and Lischer 2010), with significance determined from 10,000 permutations.

Descriptive statistics

For each locus and chameleon taxon, the number of alleles (AR), allelic size range, observed (Ho) and expected (He) heterozygosity (Nei 1987), and deviation from Hardy–Weinberg equilibrium (HWE) were estimated using ARLEQUIN. HWE was assessed using a test analogous to Fisher's exact test, based on a triangular contingency table and a modified Markov-chain random walk algorithm (Guo and Thompson 1992), with 1,000,000 Markov chains and 100,000 dememorization steps. Private allelic richness (PAR) was calculated using ADZE version 1.0 (Szpiech et al. 2008) with rarefaction to account for differences in sample size and sampling effort (Kalinowski 2005; Szpiech et al. 2008). GENEPOP ON THE WEB (Raymond and Rousset 1995; Rousset 2008) was used to test for linkage disequilibrium (LD) between loci using the log-likelihood ratio test, estimate allele frequencies, and calculate inbreeding coefficients (FIS; Weir and Cockerham 1984), which reflect the degree of inbreeding of an individual relative to the local population, with higher FIS values indicating greater inbreeding. LD tests were conducted with a dememorization of 10,000, across 100 batches of 1,000 iterations. To minimize the risk of Type I errors, p-values from tests of linkage and HWE were adjusted for multiple comparisons using Holm's sequential Bonferroni correction (Holm 1979; Rice 1989).

Results

Morphology

The datasets for both sexes were deemed robust for principal component analysis (KMO > 0.8). For females, three principal components (PCs) were extracted, accounting for 64.89% of the total variance, while four PCs were extracted for males, accounting for 72.02% of the variance (Table 1).

In females, PC1 explained >42% of the variance and had high positive loadings for all head traits (functional and ornamental), and a negative loading for tail length. PC2 was associated with proximal limb elements (TB, RD, FM) and carpal/tarsal widths, while PC3 correlated with distal limb elements (MHF, LHF, MFT, LFT). MANOVA indicated significant differences among taxa for the three PCs (Table 1). Pairwise comparisons and scatterplots showed that *Bradypodion taeniabronchum* had significantly smaller head traits (PC1) than the other species. *B. ventrale* was significantly larger for PC2 traits, i.e., proximal limb length, whereas *B. taeniabronchum* was significantly larger for PC3 traits, i.e., hand/foot size, than the other taxa (Fig. 3a, Table 2).

In males, PC1 had strong positive correlations with ornamental head traits (casque dimensions, carpal width, radius), and a negative correlation with tail length (Table 1). PC2 was associated with distal limb elements, PC3 with head traits relevant to bite force, e.g., quadrate articulation, head width/height, and PC4 with proximal hindlimb elements (TB, FM). MANOVA showed significant differences among taxa for PCs 1–3 (Table 1). Pairwise comparisons and scatterplots (Fig. 3b, Table 2) revealed that *B. ventrale* was significantly larger than both fynbos taxa for PC1 traits, e.g., casque size, head length, arm/hand dimensions, although there was no significant difference between *B.* "groendal" and *B. taeniabronchum*. The negative correlation of tail length with PC1 indicates that *B. ventrale* has a shorter tail than the two fynbos taxa. PC2 differed significantly among all taxa, with *B.* "groendal" being the smallest and *B. taeniabronchum* the largest. For PC3, *B.* "groendal" had significantly larger head width/length than *B. taeniabronchum* (Fig. 3b, Table 2).

The discriminant function analysis (DFA) showed significant differences between the group centroids for females (Table 3), consistent with the PCA and MANOVA results. Tail length was strongly and positively correlated with DF1, whereas head height and casque measurements showed strong negative correlations. These traits best discriminated among the groups. DF2 was most strongly associated with hand measurements (positive correlations). Comparisons of group centroids revealed that *B. ventrale* is distinguished by a shorter tail, but larger head traits and longer limbs (Fig. 4a). *Bradypodion taeniabronchum* is characterized by a longer tail and smaller head/ornamentation, whereas *B.* "groendal" is distinguished on DF2 by smaller hands (Fig. 4a).

Table 1. Rotated principal component matrix for the *Bradypodion ventrale* species complex, by sex, with loadings of original variables indicated for each principal component (PC) and the type of traits indicated. Also indicated is the percentage of variance (% var.) explained by each PC, and the *F* and *P* values from the multivariate analysis of variance (MANOVA). Key to abbreviations for measurements are provided in the Methods section. * indicates head traits associated with ornamentation.

Females					Males					
Type		**PC1**	**PC2**	**PC3**	**Type**		**PC1**	**PC2**	**PC3**	**PC4**
Head & tail	CHL	**0.853**	0.423	0.022	Head/ ornaments, tail & forelimbs	CHH*	**0.850**	-0.065	0.344	0.154
	HL	**0.847**	0.244	0.140		CHL	**0.770**	-0.134	0.463	0.265
	QT	**0.838**	0.148	0.097		CH*	**0.770**	-0.269	0.427	0.110
	CH*	**0.773**	0.432	-0.038		Tail	**-0.644**	0.605	-0.016	0.09
	CHH*	**0.745**	0.546	-0.009		Carpal	**0.608**	0.340	0.179	-0.081
	HW	**0.739**	0.083	0.293		RD	**0.597**	0.280	0.147	0.536
	HH	**0.541**	0.21	0.411	Distal limbs	MHF	-0.141	**0.840**	-0.021	0.08
	Tail	**-0.473**	-0.118	0.446		LHF	-0.043	**0.810**	-0.148	0.163
Proximal limb lengths & distal widths	TB	0.419	**0.809**	0.002		LFT	0.045	**0.783**	0.189	0.093
	RD	0.287	**0.791**	0.136		MFT	0.237	**0.666**	0.065	-0.027
	FM	0.125	**0.760**	0.182		HM	-0.093	**0.641**	0.207	0.468
	Carpal	0.362	**0.682**	0.158	Head lengths, width	HW	0.313	0.054	**0.806**	0.139
	Tarsal	0.158	**0.681**	0.268		HH	0.043	0.219	**0.796**	0.107
Distal limbs lengths	LHF	0.023	0.278	**0.759**		HL	0.402	-0.147	**0.713**	0.319
	MHF	0.073	0.121	**0.751**		QT	0.308	-0.100	**0.66**	0.317
	LFT	0.260	-0.064	**0.711**		Tarsal	0.402	0.215	**0.554**	-0.114
	HM	-0.022	0.336	**0.592**	Prox. limbs	FM	0.049	0.218	0.246	**0.824**
	MFT	0.231	0.39	**0.414**		TB	0.591	0.156	0.184	**0.600**
	% var.	42.803	13.815	8.271		% var.	37.033	22.096	6.881	5.922
	MANOVA					MANOVA				
	F	26.587	22.194	10.118		*F*	68.252	35.898	6.538	0.68
	P	≤ 0.001	≤ 0.001	≤ 0.001		*P*	≤ 0.001	≤ 0.001	0.002	0.508

Similarly, for males, the two discriminant functions also showed significant differences between group centroids (Table 3), again aligning with the PCA and MANOVA results. Tail and head measurements were the most influential variables on DF1 (negative correlations), while arm and hand measurements were strongly correlated with DF2. As in females, *B. ventrale* males are differentiated by a shorter tail and larger head ornamentation; *B. taeniabronchum* has the longest tail and smallest head (Fig. 4b). On DF2, *B.* "groendal" is distinguished by smaller hands and arms.

Reclassification results following cross-validation showed an overall correct classification rate above 80% for both sexes, with high within-taxon classification accuracy (Table 4), indicating that the three taxa can be reliably distinguished based on morphology.

Habitat

The regression for perch width and body size was significant for two taxa (*B. taeniabronchum* $r^2 = 0.42$, p = 0.033; *B. ventrale* $r^2 = 0.035$, p = 0.027; *B.* "groendal" $r^2 = 0.018$, p = 0.134). The non-parametric ANCOVA accounting for SVL showed significant differences in the perch widths used by the different taxa (Quade test F statistic: DFH = 2, DFE = 265, $p \leq 0.001$). *Bradypodion taeniabronchum* used the widest perches among the three taxa, and *B.* "groendal" used the narrowest. With *t* as the standardized difference between ranked group means adjusting for the covariate of SVL, the magnitude and direction of pairwise differences can be assessed (Fig. 5, Table 5): *B. ventrale* < *B. taeniabronchum*: $t = -2.413$, DF = 265, $p = 0.016$; *B. ventrale* > *B.* "groendal": $t = 2.484$, DF = 265, $p = 0.014$; *B. taeniabronchum* > *B.* "groendal": $t = 4.516$, DF = 265, $p \leq 0.001$). The regression for perch height was significant for *B. ventrale* only (*B. ventrale* $r^2 = 0.072$, p = 0.008; *B. taeniabronchum* $r^2 = 0.027$, $p = 0.132$; *B.* "groendal" $r^2 = 0.002$, $p = 0.724$). The heights at which chameleons were found perching at night also differed among taxa (Table 5), with *B.* "groendal" perching the highest and *B. taeniabronchum* the lowest, but the ANOVA and Tukey's post hoc tests showed that differences were only significant between *B. taeniabronchum* and *B.* "groendal" ($p \leq 0.001$).

The perches available in the three habitats (i.e., habitat structure) showed significant differences (Kruskal-Wallis H = 253.86, df = 2, $p \leq 0.001$), with all pairwise comparisons being significant (*B. ventrale* vs. *B. taeniabronchum*: Mann-Whitney U = 1622248.5, $p \leq 0.001$; *B. ventrale* vs. *B.* "groendal": Mann-Whitney U = 646455.5, $p \leq 0.001$; *B. taeniabronchum* vs. *B.* "groendal": Mann-Whitney

Table 2. Pairwise comparisons from the multivariate analysis of variance (MANOVA) of principal components for females (top) and males (bottom). Mean differences (I-J) show the direction and magnitude of differences. Pairwise comparisons with significant differences are indicated in bold.

	(I) Population	(J) Population	Mean Difference (I-J)	Std. Error	*P*
Females					
PC1	*B. ventrale*	*B. taeniabronchum*	1.327*	0.188	**≤ 0.001**
Head & tail		*B.* "groendal"	0.202	0.196	0.912
	B. taeniabronchum	*B. ventrale*	-1.327*	0.188	**≤ 0.001**
		B. "groendal"	-1.125*	0.213	**≤ 0.001**
	B. "groendal"	*B. ventrale*	-0.202	0.196	0.912
		B. taeniabronchum	1.125*	0.213	**≤ 0.001**
PC2	*B. ventrale*	*B. taeniabronchum*	0.871*	0.195	**≤ 0.001**
Proximal limb lengths & distal widths		*B.* "groendal"	1.278*	0.203	**≤ 0.001**
	B. taeniabronchum	*B. ventrale*	-0.871*	0.195	**≤ 0.001**
		B. "groendal"	0.407	0.220	0.202
	B. "groendal"	*B. ventrale*	-1.278*	0.203	**≤ 0.001**
		B. taeniabronchum	-0.407	0.220	0.202
PC3	*B. ventrale*	*B. taeniabronchum*	-0.732*	0.203	**≤ 0.001**
Distal limbs		*B.* "groendal"	0.230	0.212	0.843
	B. taeniabronchum	*B. ventrale*	0.732*	0.203	**≤ 0.001**
		B. "groendal"	0.962*	0.230	**≤ 0.001**
	B. "groendal"	*B. ventrale*	-0.23	0.212	0.843
		B. taeniabronchum	-0.962*	0.230	**≤ 0.001**
Males					
PC1	*B. ventrale*	*B. taeniabronchum*	1.677	0.15	**≤ 0.001**
Head, tail & forelimbs		*B.* "groendal"	1.392	0.161	**≤ 0.001**
	B. taeniabronchum	*B. ventrale*	-1.677	0.15	**≤ 0.001**
		B. "groendal"	-0.284	0.153	0.199
	B. "groendal"	*B. ventrale*	-1.392	0.161	**≤ 0.001**
		B. taeniabronchum	0.284	0.153	0.199
PC2	*B. ventrale*	*B. taeniabronchum*	-0.950	0.172	**≤ 0.001**
Distal limbs		*B.* "groendal"	0.497	0.185	**0.025**
	B. taeniabronchum	*B. ventrale*	0.950	0.172	**≤ 0.001**
		B. "groendal"	1.447	0.177	**≤ 0.001**
	B. "groendal"	*B. ventrale*	-0.497	0.185	**0.0250**
		B. taeniabronchum	-1.447	0.177	**≤ 0.001**
PC3	*B. ventrale*	*B. taeniabronchum*	0.36	0.209	0.265
Head length, width		*B.* "groendal"	-0.414	0.225	0.204
	B. taeniabronchum	*B. ventrale*	-0.36	0.209	0.265
		B. "groendal"	-0.774	0.214	**≤ 0.001**
	B. "groendal"	*B. ventrale*	0.414	0.225	0.204
		B. taeniabronchum	0.774	0.214	**≤ 0.001**
PC4	*B. ventrale*	*B. taeniabronchum*	0.221	0.217	0.930
Prox. limbs		*B.* "groendal"	0.235	0.233	0.943
	B. taeniabronchum	*B. ventrale*	-0.221	0.217	0.930
		B. "groendal"	0.014	0.222	1.000
	B. "groendal"	*B. ventrale*	-0.235	0.233	0.943
		B. taeniabronchum	-0.014	0.222	1.00

U = 2126959, $p \leq 0.001$). Overall, *B. ventrale* habitat had the widest perches, and *B.* "groendal" habitat had the narrowest perches available (Table 5).

All three taxa used significantly wider perches than the perches available to them, suggesting that chameleons choose specific perch diameters (Table 5; *B. ventrale*: Mann-Whitney U = 54761.5, $p \leq 0.001$; *B. taeniabronchum*: Mann-Whitney U = 60660, $p \leq 0.001$; *B.* "groendal": Mann-Whitney U = 31246.5, $p \leq 0.001$).

Population genetics

The *ND2* haplotype network (n = 42; Fig. 6a) revealed no haplotype sharing among taxa. However, some haplotype sharing was observed between the geographically isolated populations within *B. taeniabronchum* (Tsitsikamma and Thyspunt). Notably, haplotype reticulation occurred between the *B. taeniabronchum* population from Elandsberg and *B.* "groendal". The maximum likelihood phylogeny

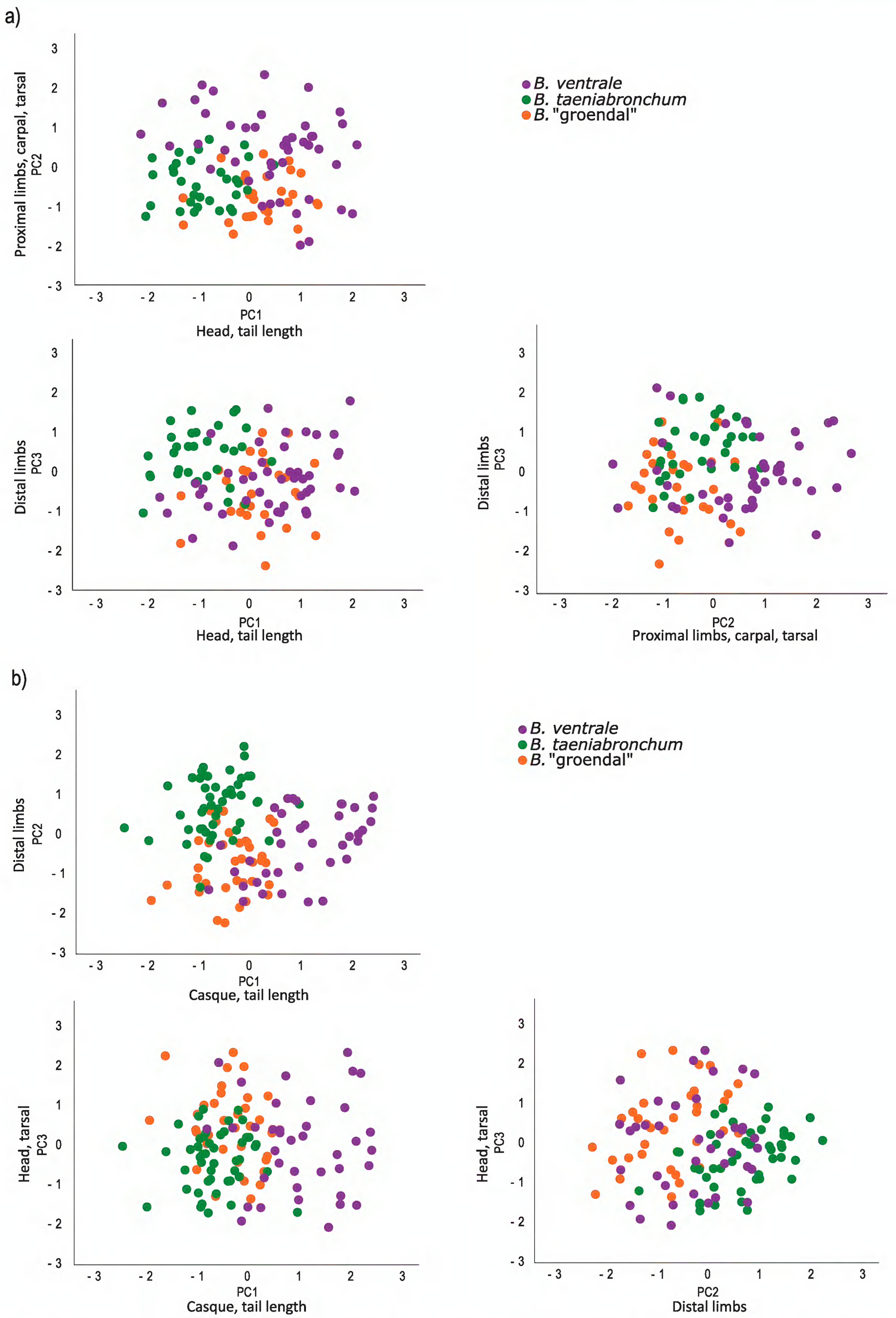

Figure 3. Scatterplots of principal component (PC) scores for **a.** Female and **b.** Male dwarf chameleons in the *Bradypodion ventrale* species complex. Original variables that loaded highest on each extracted principal component are indicated on the axes.

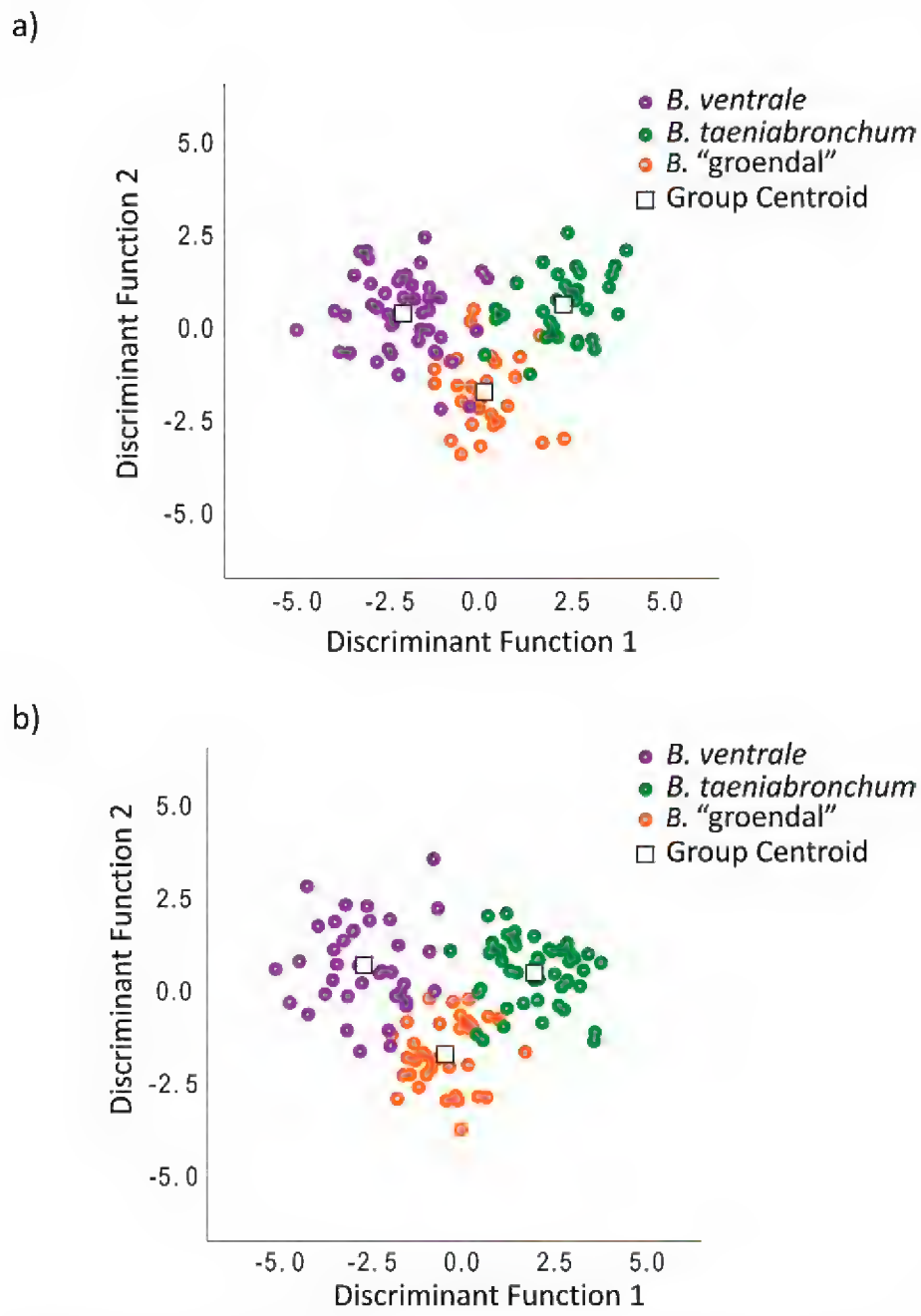

Figure 4. Scatterplot of discriminant function scores for **a.** Female and **b.** Male dwarf chameleons in the *Bradypodion ventrale* species complex. Group centroids are indicated by white squares. Discriminant Function 1 was most strongly correlated with tail length (negative correlation) and head traits (positive correlation), while Discriminant Function 2 was most strongly correlated with hand measurements (positive correlation).

Table 3. Structure matrix of the strength of correlation of variables with each discriminant function (DF) for the *Bradypodion ventrale* species complex, by sex. The highest correlations of the original variables with each discriminant function are indicated with an asterisk.

	Females			Males	
	DF1	DF2		DF1	DF2
CHL	-0.538*	0.150	CHH	-0.549*	0.230
Tail	0.485*	0.189	Tail	0.465*	0.271
ACH	-0.482*	-0.037	KHL	-0.415*	0.077
KCH	-0.472*	0.207	TB	-0.403*	0.282
TB	-0.292*	0.262	CH	-0.370*	0.045
HL	-0.270*	-0.114	QT	-0.266*	-0.122
HM	0.220*	0.19	Carpal	-0.233*	0.162
QT	-0.212*	-0.100	AHL	-0.201*	-0.071
Tarsal	-0.132*	0.111	HH	-0.150*	0.077
HH	-0.069*	-0.050	LHF	0.027	0.448*
LHF	0.263	0.586*	RD	-0.334	0.407*
MHF	0.258	0.417*	Tarsal	-0.175	0.292*
LFT	0.153	0.321*	HM	0.137	0.291*
RD	-0.220	0.288*	MHF	-0.003	0.269*
HW	-0.206	-0.222*	FM	-0.174	0.226*
Carpal	-0.152	0.220*	HW	-0.195	-0.221*
MFT	0.072	0.202*	LFT	-0.031	0.148*
FM	-0.024	0.048*	MFT	-0.102	0.116*
Eigenvalue	3.822	1.121	Eigenvalue	3.461	0.981
% Variance	77.9	22.1	% Variance	77.3	22.7
Wilks' λ	0.113	0.505	Wilks' λ	0.098	0.471
p	≤ 0.001	≤ 0.001	*p*	≤ 0.001	≤ 0.001

(Fig. 6b) was consistent with the haplotype network, showing short internal branches and weakly supported nodes within the focal clade. *Bradypodion* "groendal" lacked monophyly, and *B. taeniabronchum* was paraphyletic.

Microsatellite genotypes were generated for 144 individuals (59 *B. ventrale*, 31 *B. taeniabronchum*, 53 *B.* "groendal"; Suppl. material 1: tables S1, S4). No genotyping errors were detected; however, possible null alleles were detected at two loci (Bpu 94, Bth76) for all *B. taeniabronchum* sampled (i.e., no PCR amplification). Because the entire species was affected, it was not possible to assess the expected number of homozygotes that might exist within that group; therefore, it was deemed more appropriate to have a reduced dataset for this group (i.e., minus the two loci). *Bradypodion ventrale* was polymorphic at all 18 loci; while *B. taeniabronchum* and *B.* "groendal" individuals were polymorphic at all but one locus, Bpu238 (Table 6). Moreover, *B. taeniabronchum* showed no amplification for two loci (Bpu 94, Bth76), and thus had a reduced dataset.

Two clustering algorithms (STRUCTURE, DAPC) identified the same three genetic groups, and corresponded to the three taxa (Fig. 7). The STRUCTURE results showed some admixture between taxa (Fig. 7, Suppl. material 1: table S4). The Geneland analysis also showed the optimal population structure as five taxa, whereby *B. ventrale* is subdivided into three taxa. These same subdivisions are also apparent in the STRUCTURE output for K = 5 (Fig. 7) although the optimal STRUCTURE output was K = 3. While the substructure within *B. ventrale* is noted, it may be better explained by IBD rather than population level divergence. IBD was detected within the overall dataset (Rxy = 0.237; $R^2 = 0.056$, $p \leq 0.001$), but was essentially due to the geographic spread of samples within *B. ventrale*. When considering the taxa separately, IBD was significant for *B. ventrale* (Rxy = 0.458; $R^2 = 0.210$, $p \leq 0.001$) but not significant for the other taxa (*B. taeniabronchum*: Rxy = 0.179; $R^2 = 0.032$, $p = 0.075$; *B.* "groendal": Rxy = 0.029; $R^2 = 0.056$, $p = 0.054$).

The AMOVA (Table 7) and comparison of pairwise genetic differentiation (RST; Table 8) showed significant differences among the three taxa, further supporting their status as separate taxa, despite some admixture observed.

Descriptive statistics

Bradypodion taeniabronchum had the lowest level of overall allelic richness (AR = 11.6; Table 6), but the highest private allelic richness (PAR = 4.92; Table 9).

Table 4. Cross-validated predicted group membership from the discriminant function analysis for the *Bradypodion ventrale* species complex, by sex. Percentages of correctly classified cases are on the diagonal (bold font).

	% Predicted Group Membership		
Females	***B. ventrale***	***B. taeniabronchum***	***B. "groendal"***
B. ventrale	**80.9**	4.3	14.9
B. taeniabronchum	3.1	**87.5**	9.4
B. "groendal"	10.7	7.1	**82.1**
Males	***B. ventrale***	***B. taeniabronchum***	***B. "groendal"***
B. ventrale	**76.3**	5.3	18.4
B. taeniabronchum	2.1	**87.2**	10.6
B. "groendal"	5.7	14.3	**80.0**

Females: 83.2% of cross-validated cases correctly classified.

Males: 81.7% of cross-validated cases correctly classified.

Table 5. Descriptive statistics for perches used and perches available to chameleons in the *Bradypodion ventrale* species complex, including sample sizes (n), means (in mm or m) and standard deviation (stdev).

perch diameters used (mm)			
	n	Mean	stdev
B. ventrale	142	2.75	1.60
B. taeniabronchum	86	2.83	1.99
B. "groendal"	72	1.52	0.77
perch heights used (m)			
	n	Mean	stdev
B. ventrale	142	0.823	0.039
B. taeniabronchum	86	0.658	0.041
B. "groendal"	72	0.928	0.045
perch diameters available (mm)			
	n	Mean	stdev
B. ventrale	1336	1.79	1.54
B. taeniabronchum	3255	1.22	1.14
B. "groendal"	1426	1.08	0.88

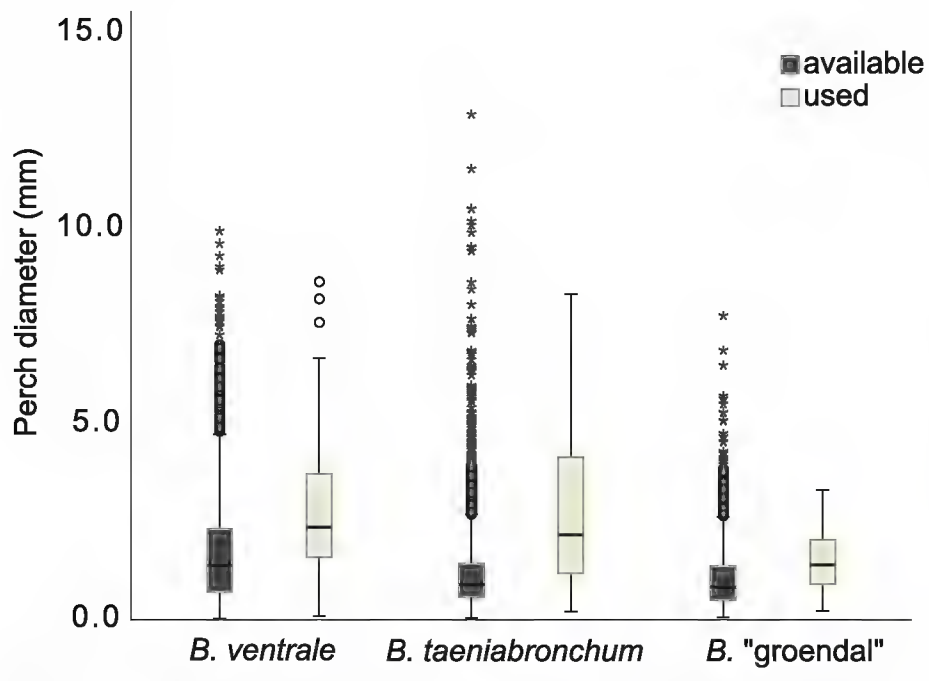

Figure 5. Box-and-whisker plot of perch widths (mm) used by chameleons from the *Bradypodion ventrale* species complex, as compared to perches available.

Bradypodion ventrale and *B.* "groendal" had similar levels of allelic richness (AR = 14.7 and 14.8, respectively; Table 6) and PAR (3.55 and 3.99, respectively; Table 9); however, *B. ventrale* was the only taxon to have private alleles at each of the 18 loci (Table 9). All taxa showed low levels of inbreeding (FIS < 0.300), with *B. taeniabronchum* having the lowest average FIS (0.147) among the three taxa (Table 6). Despite this, signatures of severe genetic bottlenecks were detected for each taxon, with average M values ranging from 0.21 to 0.27 – well below the M-value of 0.68 that is typically used as a threshold for a bottleneck. No significant linkage disequilibrium was detected across all 18 loci, even though *B. ventrale*, *B. taeniabronchum* and *B.* "groendal" showed deviations from HWE at several loci (Table 6).

Discussion

Knowledge of how differences in habitat drive phenotypic and genetic change is important in piecing together the process of ecological speciation. Convincing cases of ecological speciation require evidence of genetic and morphological differences between taxa that reflect differences in the habitats that they occupy. While gene flow between different populations can work to erode differences between them, if the ecological selective forces are strong enough, the speciation process can persist even in the presence of gene flow (e.g., Nosil 2008; Martin et al. 2013; Jónsson et al. 2014; Malinsky et al. 2018; Rutherford et al. 2018). Our results show that while there is evidence of limited ongoing or very recent gene flow between the three taxa, these taxa can still be recognisably delineated for both the mitochondrial and the nuclear genomes. Furthermore, our morphometric analysis provides support for differences between taxa for functional traits that link to habitat structure.

There was clear population structure detected among all three taxa, with no mitochondrial haplotype sharing and very low levels of nuclear allele admixture. In particular, mitochondrial haplotypes grouped according to taxa, separating *B. ventrale* and *B.* "groendal" by several mutational steps consistent with previous findings (Tolley et al. 2006). Notably, *B. taeniabronchum* is composed of three different haplogroups with two of the three sampling areas sharing haplotypes (Thyspunt Nature Reserve, Tsitsikamma Mountains), while the Elandsberg exhibits

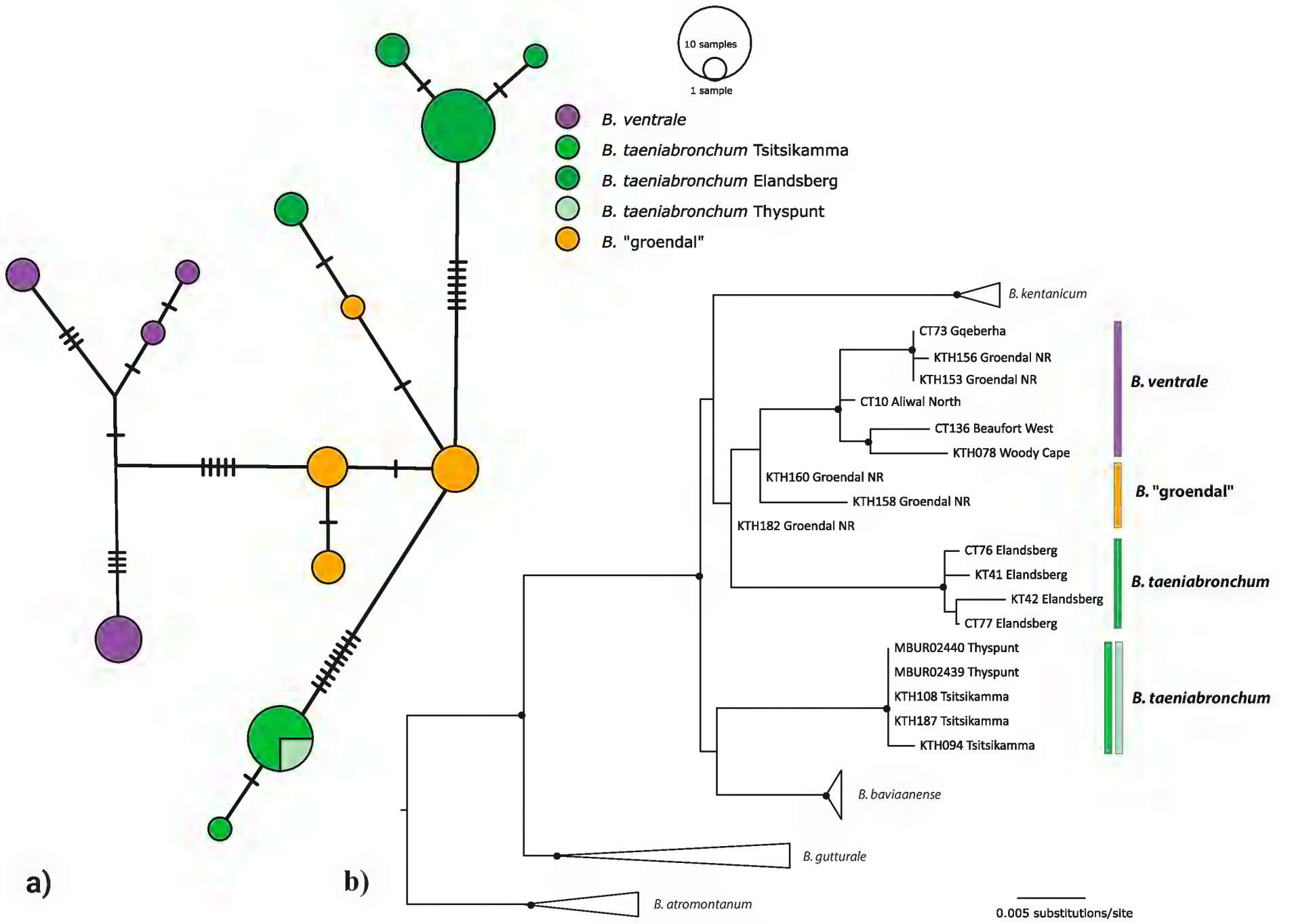

Figure 6. a. Haplotype network (ND2) of the *Bradypodion ventrale* species complex. The size of the circles is proportional to the number of individuals with that haplotype (scale provided in key), and the hatch marks along the connecting branches indicate the number of mutations between haplotypes. *Bradypodion* taxa are color-coded for each haplotype. **b.** Maximum likelihood topology for the *Bradypodion ventrale* species complex. Terminal tips for the species outside the focal taxa are collapsed, with all tips from focal taxa labeled by name (indicated by the color-coded bars), ID number, and locality. Nodes with > 70% bootstrap are indicated by the black dots. NR – Nature Reserve.

two divergent haplogroups. The three haplogroups are paraphyletic with respect to *B.* "groendal", consistent with mitochondrial gene trees that showed paraphyly of this species (e.g., Tolley et al. 2022; Fig. 6). Nevertheless, for the nuclear markers (microsatellite loci), all three localities for *B. taeniabronchum* formed a single cluster, with full support as a single taxon and no subdivision, in contrast to the mitochondrial genome. The low levels of nuclear admixture that we observed suggest that while there is some gene flow between taxa, this is unlikely to be the best explanation for the observed mitochondrial reticulation. Gene flow consistent with mitochondrial capture would likely be evident as strong introgression/admixture in the STRUCTURE plot, but this was not the case. Indeed, the nuclear genome is discordant with the mitochondrial genome for *B. taeniabronchum*. These two genomes have distinct ancestries – the former is diploid and biparentally inherited, whereas the latter is haploid and maternally inherited – and consequently, discordance is not wholly uncommon (Perea et al. 2016; Wendt et al. 2022; Stukel et al. 2023). Discordance might be attributed to the four-fold smaller effective population size of the haploid mitochondrial genome, whereby random mutations or the incorporation of foreign DNA after hybridization will sweep to fixation faster than in the nuclear genome, resulting in discordant ancestries between the nuclear and mitochondrial genomes, or in some cases, the complete 'capture' of the mitochondrial genome (Perea et al. 2016; Kunerth et al. 2022; Wright et al. 2022). Given that *B. taeniabronchum* occurs as a few isolated populations, the mitochondrial divergence that we observe is probably either due to random genetic drift sweeping to fixation in the mitochondrial genome or due to ancestral polymorphisms in the mitochondrial genome sorting incompletely among the isolated *B. taeniabronchum* lineages, causing these lineages to coalesce with *B.* "groendal" before coalescing with one another. While we expect taxa as closely related and geographically proximal as those in this study to show at least some evidence of gene flow, the weakly apparent signals of admixture in our STRUCTURE analyses could also result from incomplete lineage sorting.

Bradypodion taeniabronchum and *B.* "groendal" both occupy fynbos habitats that are similar in structure and dominated by thin, vertical perches (see also Barends et al. 2024).

Table 6. Descriptive statistics of the genetic variability for 18 microsatellite loci within the three genetic groups of the *Bradypodion ventrale* species complex, as identified by STRUCTURE and DAPC. n, number of samples; A_R, allelic richness; S, allelic size range; H_O, observed heterozygosity; H_E, expected heterozygosity; F_{IS}, Wright's inbreeding coefficient. Asterisks indicate deviations from HWE based on a Bonferroni significance value of 0.0028 ($P \leq 0.05/18$).

Locus	*B. ventrale* (n = 59)							*B. taeniabronchum* (n = 31)							*B.* "groendal" *1* (n = 54)						
	A_R	S	H_O	H_E	HWE	F_{IS}	M	A_R	S	H_O	H_E	HWE	F_{IS}	M	A_R	S	H_O	H_E	HWE	F_{IS}	M
Bpu507	8	186–224	0.33	0.76	*	0.561	0.20	11	174–220	0.69	0.85	*ns*	0.190	0.23	5	194–202	0.27	0.60	*	0.554	0.56
Bpu26	15	102–122	0.58	0.75	*ns*	0.221	0.17	21	118–214	0.93	0.95	*ns*	0.016	0.22	8	130–162	0.77	0.70	*ns*	-0.099	0.24
Bme45	16	107–175	0.64	0.89	*	0.285	0.23	20	107–195	0.67	0.95	*	0.306	0.22	19	115–187	0.83	0.92	*ns*	0.096	0.26
Bpu115	20	100–196	0.79	0.92	*	0.143	0.21	15	104–192	0.85	0.91	*ns*	0.065	0.17	19	128–208	0.91	0.92	*ns*	0.003	0.23
Bpu132	15	151–211	0.37	0.90	*	0.596	0.25	17	167–247	0.41	0.94	*	0.550	0.21	20	131–247	0.35	0.93	*	0.628	0.17
Bpu94	9	143–239	0.27	0.67	*	0.607	0.09	–	–	–	–	–	–	–	3	158–164	0.26	0.36	*ns*	0.274	0.43
Bme176	25	186–254	0.76	0.95	*	0.200	0.36	16	207–275	0.82	0.94	*	0.126	0.23	19	191–271	0.83	0.94	*ns*	0.118	0.23
Bpu238	3	108–116	0.12	0.11	*ns*	-0.043	0.33	1	112	–	–	–	–	–	1	112	–	–	–	–	–
Bth10	17	171–229	0.71	0.91	*ns*	0.220	0.29	14	153–229	0.63	0.94	*ns*	0.339	0.18	26	175–251	0.84	0.94	*ns*	0.106	0.34
Bme58	18	133–139	0.30	0.83	*	0.638	0.27	9	141–211	0.15	0.87	*	0.830	0.13	17	139–201	0.29	0.90	*	0.679	0.27
Bpu557	5	106–124	0.12	0.32	*	0.639	0.26	4	102–108	0.19	0.42	*	0.544	0.57	3	106–112	0.06	0.06	*ns*	-0.014	0.43
Bth93	7	99–147	0.60	0.65	*ns*	0.075	0.14	13	103–175	0.93	0.93	*ns*	-0.003	0.18	21	107–199	0.84	0.93	*ns*	0.095	0.23
Bme128	8	139–161	0.56	0.76	*	0.262	0.35	13	139–203	0.70	0.78	*ns*	0.101	0.20	10	137–189	0.62	0.62	*ns*	0.004	0.19
Bth76	18	101–225	0.90	0.90	*ns*	-0.004	0.14	–	–	–	–	–	–	–	17	105–209	0.60	0.91	*	0.340	0.16
Bpu577	26	172–259	0.81	0.94	*ns*	0.143	0.30	19	169–247	0.69	0.93	*	0.256	0.24	21	172–259	0.79	0.93	*ns*	0.153	0.24
Bth161	13	296–356	0.63	0.88	*	0.282	0.21	16	198–282	0.80	0.93	*ns*	0.144	0.19	20	244–376	0.36	0.91	*	0.610	0.15
Bpu184	19	242–314	0.51	0.93	*	0.456	0.26	7	255–296	0.81	0.62	*ns*	-0.321	0.17	14	242–314	0.50	0.89	*	0.445	0.19
Bpu593	23	191–263	0.84	0.93	*ns*	0.094	0.32	2	230–266	1.00	1.00	*ns*	-1.000	0.05	24	185–287	0.80	0.94	*ns*	0.144	0.23
Mean	14.7		0.55	0.78		0.299	0.24	11.6		0.68	0.86		0.142	0.21	14.8		0.58	0.79		0.243	0.27

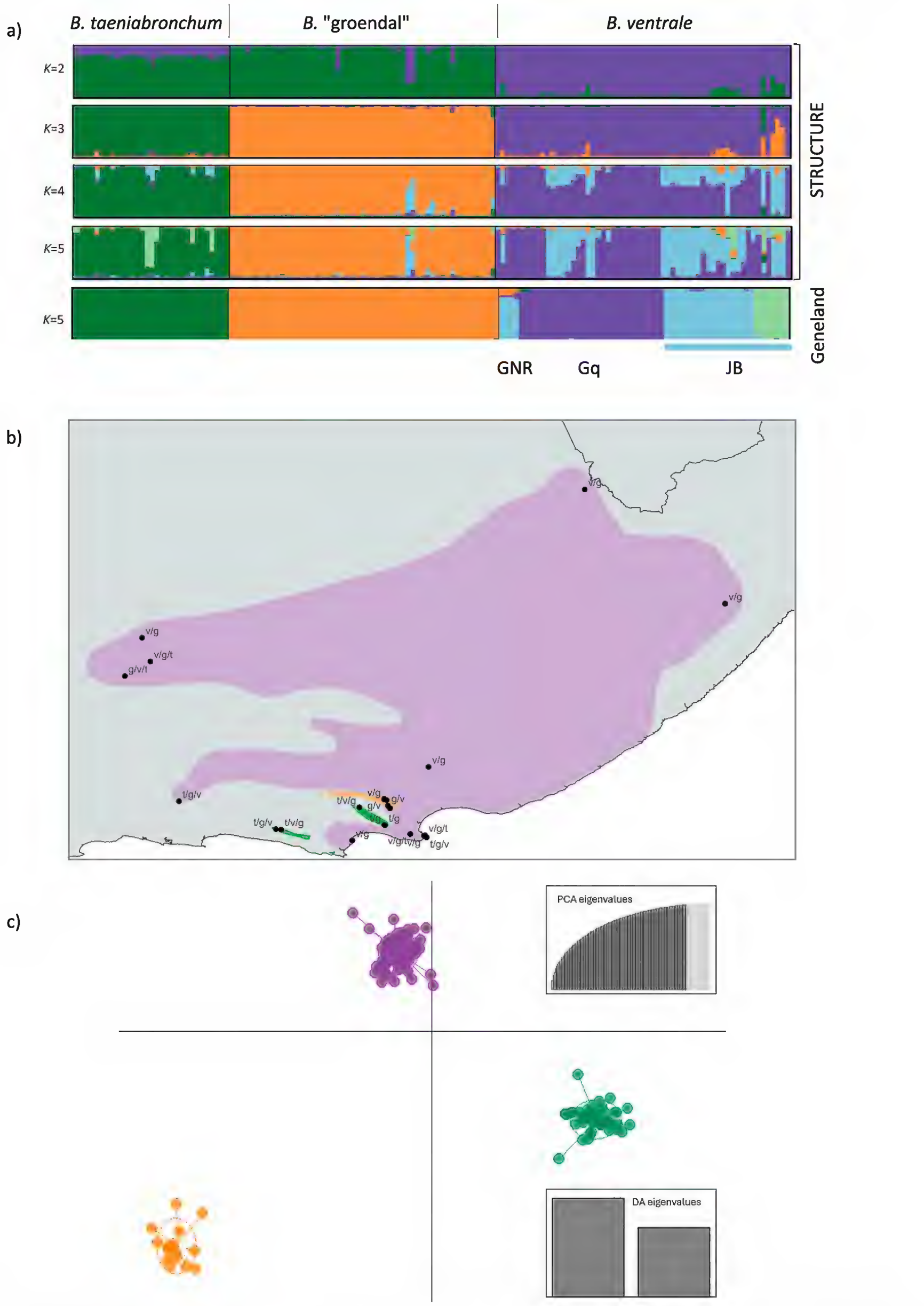

Figure 7. a. Barplots depicting genetic clusters within the *Bradypodion ventrale* species complex. The top four plots represent the STRUCTURE assignments from $K = 2–5$, with $K = 3$ being the optimal K scenario. The bottom plot illustrates the clustering assignment from Geneland with $K = 5$, whereby additional geographic structuring was found within *B. ventrale* (localities: GNR - Groendal Nature Reserve; Gq - Gqeberha; JB - Jeffreys Bay; **b.** Range maps for each taxon, with black dots indicating the localities of admixed individuals. Small letters denote the taxa that contributed to admixture (v – *B. ventrale*; t – *B. taeniabronchum*; g – *B.* "groendal", and **c.** Discriminant analysis of principal components (DAPC) plot. Three distinct clusters were identified corresponding to *Bradypodion ventrale* (purple), *B. taeniabronchum* (green), and *B.* "groendal" (orange).

Table 7. Analysis of molecular variance (AMOVA) comparing the three genetic clusters of the *Bradypodion ventrale* species complex identified using STRUCTURE and DAPC. ***$p \leq 0.001$.

Source of variation	d.f.	Sum of squares	Variance components	Percentage variation	Fixation indices
Among populations	2	345471.23	1815.59	30.89	$F_{ST} = 0.31$***
Within populations	285	1157627.54	4061.85	69.11	
Total	287	1503098.77	5877.45		

Table 8. Pairwise (R_{ST}) between the three genetic clusters (lower matrix) identified for the *Bradypodion ventrale* species complex using STRUCTURE and DAPC. ***$p \leq 0.001$.

	B. ventrale	***B. taeniabronchum***	***B. "groendal"***
B. ventrale	–		
B. taeniabronchum	0.479***	–	
B. "groendal"	0.127***	0.380***	–

In contrast, *B. ventrale* occupies a habitat that has thicker perches that are on average, less vertical (see also Barends et al. 2024). The expectation under a model of ecological speciation would be for *B. taeniabronchum* and *B.* "groendal" to converge on similar phenotypes due to occupying similar habitats, and for *B. ventrale* to differ in phenotype due to the differing habitat structure. While the taxa do converge, or diverge, as expected for most traits (e.g., most limb and head traits tend to be larger in *B. ventrale*), the pairwise pattern is more complex and differs between sexes. For example, male *B. ventrale* have larger heads (ornamentation, widths, lengths) than the fynbos species, but this pattern is not apparent for females. Given that head ornamentation plays a role in sexual signalling in chameleons (Stuart-Fox and Moussalli 2008), the disparity between sexes suggests that sexual selection is a strong selective force for males. For females, natural selection may be a stronger force of phenotypic convergence. Females of both fynbos species have small proximal limb lengths and distal limb widths, which are likely to be advantageous while gripping the narrow perch substrates characteristic of fynbos (Barends et al. 2024). In contrast, wider distal limbs for *B. ventrale* females should be advantageous in terms of gripping the larger perches that dominate their shrubby habitat, but their shorter distal limbs (e.g., foot/hand lengths) would be advantageous in this habitat as bushes are sparsely placed and chameleons must cross the ground between bushes. Indeed, other species of chameleons that utilise the ground often, or exclusively, have comparatively small distal limb elements (Herrel et al. 2013).

Although grip forces are linked to both distal and proximal limbs (Herrel et al. 2024), proximal limb elements were not different among taxa for males. Nevertheless, distal limbs (hand/feet size) were different among males, and as with females, *B. taeniabronchum* from fynbos had larger hands/feet than the other taxa. This appears to be at odds with the convergence hypothesis of functional traits related to gripping in their respective habitats, as the two fynbos species were expected to converge for all limb traits given similarity between their habitats (Barends et al. 2024). Notably however, the perches used by *B.* "groendal" were the narrowest overall, and this taxon also had the smallest distal limb sizes. In contrast, *B. taeniabronchum* used the widest perches overall. Despite the two fynbos habitats having similar perch structure overall, *B. taeniabronchum* selected larger perches than the mean size available, and this could be a major driver of their larger distal limbs. There are at least two plausible explanations for this result – either individuals typically perch very low on bushes where side branches are likely to be thicker than the tops, or they preferentially chose plant species that have larger perches. Indeed, our results show that *B. taeniabronchum* does perch significantly lower than the other two taxa, but our anecdotal observations suggest the latter might also be important, whereby many individuals sampled were often perched on the thick stem of sedges. The question remains as to why they chose large perches, but it may relate to other environmental conditions of the mountains where these chameleons were sampled. Our *ad hoc* observations are that these sites are much more windy and generally stormy than the mountains where *B.* "groendal" occurs, and if so, *B. taeniabronchum* may need to seek shelter lower in bushes and/or grasp more stable stems.

Overall, different lines of evidence (ecology, morphology and genetics) show notable differences among taxa (Table 10), fitting a model of ecological speciation. The fynbos taxa from analogous habitats have converged on a similar phenotype, despite some deviations from the primary pattern. In contrast, the habitat of *B. ventrale* differs in terms of structure, and this taxon generally shows morphological divergence from the fynbos taxa. The DFA suggests, however, that all three taxa can be reliably classified by differing combinations of functional morphological traits, and while there is some minor allele sharing, there are significant genetic differences for both nuclear and mitochondrial genes.

The overall evidence supports a model of ecological speciation for these taxa of *Bradypodion*, either in the presence of gene flow or with shared ancestral alleles persisting in the taxa. Indeed, it has generally been accepted that many species share some alleles, but also that gene flow can persist long after speciation, even despite chromosomal rearrangements between species (Jónsson et al. 2014). The mounting evidence suggests that the speciation process can occur in the presence of gene flow, with diverging populations exchanging genes, but with the lineages nevertheless being on different evolutionary trajectories (Martin et al. 2013; Rutherford et al. 2018; Liu et al. 2020). While lineage sorting is incomplete among these *Bradypodion*, the total evidence suggests they are indeed on different evolutionary trajectories and can be considered distinct species.

Table 9. Private allelic richness (PA_R) across the 18 microsatellite loci for each of the three genetic clusters within the *Bradypodion ventrale* species complex. '–' indicates no data for this locus due to non-amplification for all individuals in the cluster.

Locus Genetic Cluster	Bpu 507	Bpu 26	Bme 45	Bpu 115	Bpu 132	Bpu 94	Bme 176	Bpu 238	Bth 10	Bme 58	Bpu 557	Bth 93	Bme 128	Bth 76	Bpu 577	Bth 161	Bpu 184	Bpu 593	Mean	Variance	SE
B. ventrale	1.13	2.77	1.34	3.71	3.06	6.26	6.81	1.03	3.69	3.06	1.05	1.25	0.56	6.82	4.19	5.05	6.00	6.07	3.55	4.85	0.52
B. taeniabronchum	6.20	8.62	3.55	5.54	3.18	–	4.01	0	9.87	4.32	1.90	2.48	5.64	–	4.05	12.74	1.70	0	4.92	11.31	0.87
B. "groendal"	0.19	1.16	1.20	3.05	4.51	0	3.73	0	7.95	5.60	0.34	5.10	1.60	6.89	3.23	8.19	3.95	7.18	3.99	7.12	0.67

Table 10. Lines of evidence (ecology, morphology and genetics) showing differences among taxa of *Bradypodion*.

Population	Habitat Type	Perch Use	Habitat Structure	Morphology (Females)	Morphology (Males)	Genetics
B. ventrale	shrub	uses intermediate perch height and diameter	largest perch diameters available	longest limbs, shortest tail	largest head ornamentation traits, shortest tail	unique mitochondrial haplotypes; shares microsatellite alleles with *B.* "groendal"
B. taeniabronchum	fynbos	uses lowest and widest perches	intermediate perch diameters available	largest hands/feet, smallest head traits	largest hands/feet, smallest head traits	unique mitochondrial haplotypes; shares alleles with both *B. ventrale* and *B.* "groendal"
B. "groendal"	fynbos	uses highest and narrowest perches	narrowest perch diameters available	intermediate morphology	smallest hands/feet, large heads (non-ornamentation traits)	unique mitochondrial haplotypes; shares microsatellite alleles with *B. ventrale*

Acknowledgements

This work was funded by the National Research Foundation of South Africa, Dimensions of Biodiversity Program (Grant no. 136381). Ethical clearance was approved by the Animal Research and Ethics Committees of the University of Johannesburg (ethical clearance no. 2019-10-10), and the South African National Biodiversity Institute (0003-20110, 0001-2013, 0001-2015). Permits to conduct fieldwork were granted by the Eastern Cape Economic Development, Environmental Affairs and Tourism Board (RSH 07/2023, RSH 24/2021, WRO 41/03WR; WRO 15/03WR, CRO 3/19CR, CRO 35/15CR, CRO 36/15CR, CRO 32/20CR, CRO 33/20CR), and a Threatened or Protected Species Standing Permit #S65803. We thank the many students, interns, research colleagues, and other volunteers who assisted on the many field trips associated with this project, as well as the insightful and helpful comments provided by three anonymous reviewers.

References

Aljanabi SM, Martinez I (1997) Universal and rapid salt-extraction of high quality genomic DNA for PCR-based techniques. Nucleic Acids Research 25(22): 4692–4693. https://doi.org/10.1093/nar/25.22.4692

Aurelle D, Ledoux J-B (2013) Interplay between isolation by distance and genetic clusters in the red coral *Corallium rubrum*: Insights from simulated and empirical data. Conservation Genetics 14(3): 705–716. https://doi.org/10.1007/s10592-013-0464-0

Ball MC, Finnegan L, Manseau M, Wilson P (2010) Integrating multiple analytical approaches to spatially delineate and characterize genetic population structure: An application to boreal caribou (*Rangifer tarandus caribou*) in central Canada. Conservation Genetics 11(6): 2131–2143. https://doi.org/10.1007/s10592-010-0099-3

Barends JM, Tolley KA (2024) Big cities, big bodies: urbanisation correlates with large body sizes and enhanced body condition in African dwarf chameleons (Genus: *Bradypodion*). African Zoology 59(3): 145–153. https://doi.org/10.1080/15627020.2024.2402256

Barends JM, Petford MA, Tolley KA (2024) Comparing perch availability and perch use between African dwarf chameleon (*Bradypodion*) ecomorphs. Current Zoology 2024: zoae076. https://doi.org/10.1093/cz/zoae076

Bermingham E, Rohwert S, Freeman S, Woodt C (1992) Vicariance and biogeography in the Pleistocene and speciation in North American wood warblers: A test of Mengel's model. Proceedings of the National Academy of Sciences of the United States of America 89(14): 6624–6628. https://doi.org/10.1073/pnas.89.14.6624

Blair C, Weigel DE, Balazik M, Keeley ATH, Walker FM, Landguth E, Cushman S, Murphy M, Waits L, Balkenhol N (2012) A simulation-based evaluation of methods for inferring linear barriers to gene flow. Molecular Ecology Resources 12(5): 822–833. https://doi.org/10.1111/j.1755-0998.2012.03151.x

Brookfield JFY (1996) A simple new method for estimating null allele frequency from heterozygote deficiency. Molecular Ecology 5(3): 453–455. https://doi.org/10.1111/j.1365-294X.1996.tb00336.x

Butlin RK, Tregenza T (1997) Is speciation no accident? Nature 387(6633): 551–553. https://doi.org/10.1038/42355

Campbell-Staton SC, Winchell KM, Rochette NC, Fredette J, Maayan I, Schweizer RM, Catchen J (2020) Parallel selection on thermal physiology facilitates repeated adaptation of city lizards to urban heat islands. Nature Ecology & Evolution 4(4): 652–658. https://doi.org/10.1038/s41559-020-1131-8

Ceccarelli FS, Menegon M, Tolley KA, Tilbury CR, Gower DJ, Laserna MH, Kasahun R, Rodriguez-Prieto A, Hagmann R, Loader SP (2014) Evolutionary relationships, species delimitation and biogeography of Eastern Afromontane horned chameleons (Chamaeleonidae: *Trioceros*). Molecular Phylogenetics and Evolution 80: 125–136. https://doi.org/10.1016/j.ympev.2014.07.023

Chapuis M-P, Estoup A (2007) Microsatellite null alleles and estimation of population differentiation. Molecular Biology and Evolution 24(3): 621–631. https://doi.org/10.1093/molbev/msl191

Coyne JA, Orr HA (1989) Patterns of speciation in Drosophila. Evolution 43(2): 362–381. https://doi.org/10.1111/j.1558-5646.1989.tb04233.x

Crase B, Liedloff A, Vesk PA, Fukuda Y, Wintle BA (2014) Incorporating spatial autocorrelation into species distribution models alters forecasts of climate-mediated range shifts. Global Change Biology 20(8): 2566–2579. https://doi.org/10.1111/gcb.12598

Crisp MD, Trewick SA, Cook LG (2011) Hypothesis testing in biogeography. Trends in Ecology & Evolution 26(2): 66–72. https://doi.org/10.1016/j.tree.2010.11.005

da Silva JM, Tolley KA (2013) Ecomorphological variation and sexual dimorphism in a recent radiation of dwarf chameleons (*Bradypodion*). Biological Journal of the Linnean Society. Linnean Society of London 109(1): 113–130. https://doi.org/10.1111/bij.12045

da Silva JM, Tolley KA (2017) Diversification through ecological opportunity in dwarf chameleons. Journal of Biogeography 44(4): 834–847. https://doi.org/10.1111/jbi.12966

Dasmahapatra KK, Lamas G, Simpson F, Mallet J (2010) The anatomy of a "suture zone" in Amazonian butterflies: A coalescent-based test for vicariant geographic divergence and speciation. Molecular Ecology 19(19): 4283–4301. https://doi.org/10.1111/j.1365-294X.2010.04802.x

de Queiroz K (2005) A unified concept of species and its consequences for the future of taxonomy. Proceedings of the California Academy of Sciences, 56, Suppl. 1, No. 18: 196–215.

Dufresnes C, Nicieza AG, Litvinchuk SN, Rodrigues N, Jeffries DL, Vences M, Perrin N, Martínez-Solano Í (2020) Are glacial refugia hotspots of speciation and cytonuclear discordances? Answers from the genomic phylogeography of Spanish common frogs. Molecular Ecology 29(5): 986–1000. https://doi.org/10.1111/mec.15368

Earl DA, von Holdt BM (2012) STRUCTURE HARVESTER: A website and program for visualizing STRUCTURE output and implementing the Evanno method. Conservation Genetics Resources 4(2): 359–361. https://doi.org/10.1007/s12686-011-9548-7

Evanno G, Regnaut S, Goudet J (2005) Detecting the number of clusters of individuals using the software STRUCTURE: A simulation study. Molecular Ecology 14(8): 2611–2620. https://doi.org/10.1111/j.1365-294X.2005.02553.x

Excoffier L, Lischer H (2010) Arlequin suite ver 3.5: A new series of programs to perform population genetics analyses under Linux and Windows. Molecular Ecology Resources 10(3): 564–567. https://doi.org/10.1111/j.1755-0998.2010.02847.x

Falush D, Stephens M, Pritchard JK (2003) Inference of population structure using multilocus genotype data: Linked loci and correlated allele frequencies. Genetics 164(4): 1567–1587. https://doi.org/10.1093/genetics/164.4.1567

Feldheim KA, Chauke L, Hopkins K, Tolley KA (2010) Characterization of microsatellite loci from a South African endemic, the Cape Dwarf Chameleon (*Bradypodion pumilum*). Conservation Genetics Resources 2(S1): 165–168. https://doi.org/10.1007/s12686-009-9108-6

Feldheim K, da Silva J, Tolley KA (2012) Isolation of novel microsatellite loci in dwarf chameleons from KwaZulu-Natal Province, South Africa and their cross-amplification in other *Bradypodion* species. Conservation Genetics Resources 4(1): 205–211. https://doi.org/10.1007/s12686-011-9472-x

Frantz AC, Cellina S, Krier A, Schley L, Burke T (2009) Using spatial Bayesian methods to determine the genetic structure of a continuously distributed population: Clusters or isolation by distance? Journal of Applied Ecology 46(2): 493–505. https://doi.org/10.1111/j.1365-2664.2008.01606.x

Guillot G, Mortier F, Estoup A (2005) GENELAND: A computer package for landscape genetics. Molecular Ecology Notes 5(3): 712–715. https://doi.org/10.1111/j.1471-8286.2005.01031.x

Guillot G, Santos F, Estoup A (2008) Analysing georeferenced population genetics data with Geneland: A new algorithm to deal with null alleles and a friendly graphical user interface. Bioinformatics (Oxford, England) 24(11): 1406–1407. https://doi.org/10.1093/bioinformatics/btn136

Guo S, Thompson E (1992) Performing the exact test of Hardy-Weinberg proportion for multiple alleles. Biometrics 48(2): 361–372. https://doi.org/10.2307/2532296

Harshman J, Braun EL, Braun MJ, Huddleston CJ, Bowie RCK, Chojnowski JL, Hackett SJ, Han K-L, Kimball RT, Marks BD, Miglia KJ, Moore WS, Reddy S, Sheldon FH, Steadman DW, Steppan SJ, Witt CC, Yuri T (2008) Phylogenomic evidence for multiple losses of flight in ratite birds. Proceedings of the National Academy of Sciences of the United States of America 105(36): 13462–13467. https://doi.org/10.1073/pnas.0803242105

Hendry AP (2009) Ecological speciation! Or the lack thereof? Canadian Journal of Fisheries and Aquatic Sciences 66(8): 1383–1398. https://doi.org/10.1139/F09-074

Herrel A, Measey GJ, Vanhooydonck B, Tolley KA (2011) Functional consequences of morphological differentiation between populations of the Cape Dwarf Chameleon (*Bradypodion pumilum*). Biological Journal of the Linnean Society. Linnean Society of London 104(3): 692–700. https://doi.org/10.1111/j.1095-8312.2011.01764.x

Herrel A, Tolley KA, Measey GJ, da Silva JM, Potgieter DF, Biostel R, Vanhooydonck B (2013) Slow but tenacious: An analysis of running and gripping performance in chameleons. The Journal of Experimental Biology 216: 1025–1030. https://doi.org/10.1242/jeb.078618

Herrel A, Taft JM, Main DC, da Silva JM, Tolley KA (2024) Branching out: Perch diameter and orientation affect pull strength in chameleons (Genus: *Bradypodion*). Biological Journal of the Linnean Society. Linnean Society of London 143(3): blae003. https://doi.org/10.1093/biolinnean/blae003

Hewitt GM (1996) Some genetic consequences of ice ages, and their role, in divergence and speciation. Biological Journal of the Linnean Society. Linnean Society of London 58(3): 247–276. https://doi.org/10.1006/bijl.1996.0035

Holm S (1979) A simple sequential rejective multiple test procedure. Scandinavian Journal of Statistics, Theory and Applications 6: 65–70. https://www.jstor.org/stable/4615733

Hoorn C, Wesselingh FP, Ter Steege H, Bermudez MA, Mora A, Sevink J, Sanmartín I, Sanchez-Meseguer A, Anderson CL, Figueiredo JP, Jaramillo C, Riff D, Negri FR, Hooghiemstra H, Lundberg J, Stadler T, Särkinen T, Antonelli A (2010) Amazonia through time: Andean uplift, climate change, landscape evolution, and biodiversity. Science 330(6006): 927–931. https://doi.org/10.1126/science.1194585

Hopkins KP, Tolley KA (2011) Morphological variation in the Cape Dwarf Chameleon (*Bradypodion pumilum*) as a consequence of spatially explicit habitat structure differences. Biological Journal of the Linnean Society. Linnean Society of London 102(4): 878–888. https://doi.org/10.1111/j.1095-8312.2011.01618.x

Hoskin CJ, Higgie M, McDonald KR, Moritz C (2005) Reinforcement drives rapid allopatric speciation. Nature 437(7063): 1353–1356. https://doi.org/10.1038/nature04004

Jakobsson M, Rosenberg NA (2007) CLUMPP: A cluster matching and permutation program for dealing with label switching and multimodality in analysis of population structure. Bioinformatics (Oxford, England) 23(14): 1801–1806. https://doi.org/10.1093/bioinformatics/btm233

Jombart T (2008) adegenet: A R package for the multivariate analysis of genetic markers. Bioinformatics (Oxford, England) 24(11): 1403–1405. https://doi.org/10.1093/bioinformatics/btn129

Jombart T, Devillard S, Balloux F (2010) Discriminant analysis of principal components: A new method for the analysis of genetically structured populations. BMC Genetics 11(1): 94. https://doi.org/10.1186/1471-2156-11-94

Jónsson H, Schubert M, Seguin-Orlando A, Ginolhac A, Petersen L, Fumagalli M, Albrechtsen A, Petersen B, Korneliussen TS, Vilstrup JT, Lear T, Myka JL, Lundquist J, Miller DC, Alfarhan AH, Alquraishi SA, Al-Rasheid KAS, Stagegaard J, Strauss G, Bertelsen MF, Sicheritz-Ponten T, Antczak DF, Bailey E, Nielsen R, Willerslev E, Orlando L (2014) Speciation with gene flow in equids despite extensive chromosomal plasticity. Proceedings of the National Academy of Sciences of the United States of America 111(52): 18655–18660. https://doi.org/10.1073/pnas.1412627111

Kalinowski ST (2005) HP-RARE 10: A computer program for performing rarefaction on measures of allelic richness. Molecular Ecology Notes 5(1): 187–189. https://doi.org/10.1111/j.1471-8286.2004.00845.x

Kunerth HD, Tapisso JT, Valente R, Mathias M da L, Alves PC, Searle JB, Vega R, Paupério J (2022) Characterising Mitochondrial Capture in an Iberian Shrew. Genes 13(12): 2228. https://doi.org/10.3390/genes13122228

Lancaster LT, Dudaniec RY, Hansson B, Svensson EI (2015) Latitudinal shift in thermal niche breadth results from thermal release during a climate-mediated range expansion. Journal of Biogeography 42(10): 1953–1963. https://doi.org/10.1111/jbi.12553

Leigh JW, Bryant D (2015) PopART: Full-feature software for haplotype network construction. Methods in Ecology and Evolution 6(9): 1110–1116. https://doi.org/10.1111/2041-210X.12410

Liu X, Glémin S, Karrenberg S (2020) Evolution of putative barrier loci at an intermediate stage of speciation with gene flow in campions (Silene). Molecular Ecology 29(18): 3511–3525. https://doi.org/10.1111/mec.15571

Losos JB, Warheit KI, Schoener TW (1997) Adaptive differentiation following experimental island colonization in *Anolis* lizards. Nature 387(6628): 70–73. https://doi.org/10.1038/387070a0

Losos JB, Jackman TR, Larson A, de Queiroz K, Rodriguez-Schnettino L (1998) Contingency and determinism in replicated adaptive radiations of island lizards. Science (1979) 279: 2115–2117. https://doi.org/10.1126/science.279.5359.2115

Malinsky M, Svardal H, Tyers AM, Miska EA, Genner MJ, Turner GF, Durbin R (2018) Whole-genome sequences of Malawi cichlids reveal multiple radiations interconnected by gene flow. Nature Ecology & Evolution 2(12): 1940–1955. https://doi.org/10.1038/s41559-018-0717-x

Martin SH, Dasmahapatra KK, Nadeau NJ, Salazar C, Walters JR, Simpson F, Blaxter M, Manica A, Mallet J, Jiggins CD (2013) Genome-wide evidence for speciation with gene flow in *Heliconius* butterflies. Genome Research 23(11): 1817–1828. https://doi.org/10.1101/gr.159426.113

Macey JR, Larson A, Ananjeva NB, Papenfuss TJ (1997a) Evolutionary shifts in three major structural features of the mitochondrial genome among iguanian lizards. Journal of Molecular Evolution 44: 660–674. https://doi.org/10.1007/PL00006190

Macey JR, Larson A, Ananjeva NB, Fang ZL, Papenfuss TJ (1997b) Two novel gene orders and the role of light-strand replication in rearrangement of the vertebrate mitochondrial genome. Molecular Biology and Evolution 14: 91–104. https://doi.org/10.1093/oxfordjournals.molbev.a025706

Miller MA, Pfeiffer W, Schwartz T (2010) Creating the CIPRES Science Gateway for inference of large phylogenetic trees. In: Proceedings of the Gateway Computing Environments Workshop (GCE), 14 November 2010, New Orleans, 1–8. https://doi.org/10.1109/GCE.2010.5676129

Musher LJ, Ferreira M, Auerbach AL, McKay J, Cracraft J (2019) Why is Amazonia a "source" of biodiversity? Climate-mediated dispersal and synchronous speciation across the Andes in an avian group (Tityrinae). Proceedings. Biological Sciences 286(1900): 20182343. https://doi.org/10.1098/rspb.2018.2343

Nei M (1987) Molecular Evolutionary Genetics. Columbia University Press, New York, 512 pp. https://doi.org/10.7312/nei-92038

Nosil P (2008) Speciation with gene flow could be common. Molecular Ecology 17(9): 2103–2106. https://doi.org/10.1111/j.1365-294X.2008.03715.x

Öhlund G, Bodin M, Nilsson KA, Öhlund SO, Mobley KB, Hudson AG, Peedu M, Brännström Å, Bartels P, Præbel K, Hein CL, Johansson P, Englund G (2020) Ecological speciation in European whitefish is driven by a large-gaped predator. Evolution Letters 4(3): 243–256. https://doi.org/10.1002/evl3.167

Peakall ROD, Smouse PE (2006) GenAlEx 6: Genetic analysis in Excel. Population genetic software for teaching and research. Molecular Ecology Notes 6(1): 288–295. https://doi.org/10.1111/j.1471-8286.2005.01155.x

Perea S, Vukić J, Šanda R, Doadrio I (2016) Ancient mitochondrial capture as factor promoting mitonuclear discordance in freshwater fishes: A case study in the genus *Squalius* (Actinopterygii, Cyprinidae) in Greece. PLoS One 11(12): e0166292. https://doi.org/10.1371/journal.pone.0166292

Petford MA, Herrel A, Alexander GJ, Tolley KA (2024) Differences between urban and natural populations of dwarf chameleons (*Bradypodion damaranum*): A case of urban warfare. Urban Ecosystems 27(2): 577–589. https://doi.org/10.1007/s11252-023-01474-1

Pritchard JK, Stephens M, Donnelly P (2000) Inference of population structure using multilocus genotype data. Genetics 155(2): 945–959. https://doi.org/10.1093/genetics/155.2.945

Raymond M, Rousset F (1995) GENEPOP (version 1.2): Population genetics software for exact tests and ecumenicism. The Journal of Heredity 86(3): 248–249. https://doi.org/10.1093/oxfordjournals.jhered.a111573

Reznick DN, Losos J, Travis J (2019) From low to high gear: There has been a paradigm shift in our understanding of evolution. Ecology Letters 22(2): 233–244. https://doi.org/10.1111/ele.13189

Rice WR (1989) Analyzing tables of statistical tests. Evolution; International Journal of Organic Evolution 43(1): 223–225. https://doi.org/10.2307/2409177

Rice WR, Hostert EE (1993) Laboratory experiments on speciation: what have we learned in 40 years? Evolution 47(6):1637–1653. https://doi.org/10.1111/j.1558-5646.1993.tb01257.x

Rincón-Barrado M, Olsson S, Villaverde T, Moncalvillo B, Pokorny L, Forrest A, Riina R, Sanmartín I (2021) Ecological and geological processes impacting speciation modes drive the formation of wide-range disjunctions within tribe Putorieae (Rubiaceae). Journal of Systematics and Evolution 59(5): 915–934. https://doi.org/10.1111/jse.12747

Roques S, Duchesne P, Bernatchez L (1999) Potential of microsatellites for individual assignment: The North Atlantic redfish (genus *Sebastes*) species complex as a case study. Molecular Ecology 8(10): 1703–1717. https://doi.org/10.1046/j.1365-294x.1999.00759.x

Rosenberg NA (2004) Distruct: A program for the graphical display of population structure. Molecular Ecology Notes 4(1): 137–138. https://doi.org/10.1046/j.1471-8286.2003.00566.x

Rousset F (2008) Genepop'007: A complete reimplementation of the Genepop software for Windows and Linux. Molecular Ecology Resources 8(1): 103–106. https://doi.org/10.1111/j.1471-8286.2007.01931.x

Rundell RJ, Price TD (2009) Adaptive radiation, nonadaptive radiation, ecological speciation and nonecological speciation. Trends in Ecology & Evolution 24(7): 394–399. https://doi.org/10.1016/j.tree.2009.02.007

Rutherford S, Rossetto M, Bragg JG, McPherson H, Benson D, Bonser SP, Wilson PG (2018) Speciation in the presence of gene flow: Population genomics of closely related and diverging *Eucalyptus* species. Heredity 121(2): 126–141. https://doi.org/10.1038/s41437-018-0073-2

Rutledge LY, Garroway CJ, Loveless KM, Patterson BR (2010) Genetic differentiation of eastern wolves in Algonquin Park despite bridging gene flow between coyotes and grey wolves. Heredity 105(6): 520–531. https://doi.org/10.1038/hdy.2010.6

Sanmartín I, Ronquist F (2004) Southern hemisphere biogeography inferred by event-based models: Plant versus animal patterns. Systematic Biology 53(2): 216–243. https://doi.org/10.1080/10635150490423430

Schluter D (2009) Evidence for ecological speciation and its alternative. Science 323(5915): 737–741. https://doi.org/10.1126/science.1160006

Schwartz MK, McKelvey KS (2009) Why sampling scheme matters: The effect of sampling scheme on landscape genetic results. Conservation Genetics 10(2): 441–452. https://doi.org/10.1007/s10592-008-9622-1

Smith A (1831) Contributions to the natural history of South Africa, No. 1. South African Quarterly Journal 1(5): 9–24.

Stamatakis A (2014) RAxML version 8: A tool for phylogenetic analysis and post-analysis of large phylogenies. Bioinformatics (Oxford, England) 30(9): 1312–1313. https://doi.org/10.1093/bioinformatics/btu033

Stuart-Fox D, Moussalli A (2008) Selection for social signalling drives the evolution of chameleon colour change. PLoS Biology 6(1): e25. https://doi.org/10.1371/journal.pbio.0060025

Stukel M, Porczak AE, Gordon ERL, Vailionis J, Haji D, Buckley TR, Lemmon AR, Lemmon EM, Simon C (2023) Phylogenomics improves the phylogenetic resolution and provides strong evidence of mito-nuclear discordance in two genera of a New Zealand cicada (Hemiptera: Cicadidae) species radiation. Systematic Entomology. https://doi.org/10.1111/syen.12613

Svensson EI (2012) Non-ecological speciation, niche conservatism and thermal adaptation: How are they connected? Organisms, Diversity & Evolution 12(3): 229–240. https://doi.org/10.1007/s13127-012-0082-6

Szpiech ZA, Jakobsson M, Rosenberg NA (2008) ADZE: A rarefaction approach for counting alleles private to combinations of populations. Bioinformatics (Oxford, England) 24(21): 2498–2504. https://doi.org/10.1093/bioinformatics/btn478

Tabachnick BG, Fidell LS (2019) Using Multivariate Statistics, 7th edition. Pearson, Boston, MA, 1024 pp.

Tolley KA, Burger M (2007) Chameleons of Southern Africa. Struik Publishers, Cape Town, 100 pp.

Tolley KA, Tilbury CR, Branch WR, Matthee CA (2004) Phylogenetics of the southern African dwarf chameleons, *Bradypodion* (Squamata: Chamaeleonidae). Molecular Phylogenetics and Evolution 30(2): 354–365. https://doi.org/10.1016/S1055-7903(03)00211-2

Tolley KA, Burger M, Turner AA, Matthee CA (2006) Biogeographic patterns and phylogeography of dwarf chameleons (*Bradypodion*) in an African biodiversity hotspot. Molecular Ecology 15(3): 781–793. https://doi.org/10.1111/j.1365-294X.2006.02836.x

Tolley KA, Chase BM, Forest F (2008) Speciation and radiations track climate transitions since the Miocene Climatic Optimum: a case study of southern African chameleons. Journal of Biogeography 35(8): 1402–1414. https://doi.org/10.1111/j.1365-2699.2008.01889.x

Tolley KA, Townsend TM, Vences M (2013) Large-scale phylogeny of chameleons suggests African origins and Eocene diversification. Proceedings of the Royal Society of London, Series B 280(1759): 20130184. https://doi.org/10.1098/rspb.2013.0184

Tolley KA, Hopkins KP, da Silva JM (2019) Genetic structure associated with habitat diversification supports the independent evolution of ecomorphs in *Bradypodion pumilum*. African Journal of Herpetology 68(1): 77–89. https://doi.org/10.1080/21564574.2019.1646324

Tolley KA, Burger M, Tilbury CR (2022) Convergence and vicariance: Speciation of chameleons in the Cape Fold Mountains, South Africa, and the description of three new species of *Bradypodion* Fitzinger, 1843. African Journal of Herpetology 71(1): 14–38. https://doi.org/10.1080/21564574.2021.1998236

Tucker JM, Schwartz MK, Truex RL, Wisely SM, Allendorf FW (2014) Sampling affects the detection of genetic subdivision and conservation implications for fisher in the Sierra Nevada. Conservation Genetics 15(1): 123–136. https://doi.org/10.1007/s10592-013-0525-4

Van Oosterhout C, Hutchinson WF, Wills DP, Shipley P (2004) MICRO-CHECKER: software for identifying and correcting genotyping errors in microsatellite data. Molecular Ecology Notes 4(3): 535–538. https://doi.org/10.1111/j.1471-8286.2004.00684.x

Weir BS, Cockerham CC (1984) Estimating F-statistics for the analysis of population-structure. Evolution; International Journal of Organic Evolution 38(6): 1358–1370. https://doi.org/10.2307/2408641

Wendt M, Kulanek D, Varga Z, Rákosy L, Schmitt T (2022) Pronounced mito-nuclear discordance and various Wolbachia infections in the water ringlet Erebia pronoe have resulted in a complex phylogeographic structure. Scientific Reports 12(1): 5175. https://doi.org/10.1038/s41598-022-08885-8

Winchell KM, Campbell-Staton SC, Losos JB, Revell LJ, Verrelli BC, Geneva AJ (2023) Genome-wide parallelism underlies contemporary adaptation in urban lizards. Proceedings of the National Academy of Sciences of the United States of America 120(3): e2216789120. https://doi.org/10.1073/pnas.2216789120

Wright EA, Roberts EK, Platt RN, Bayouth JV, Conway WC, Bradley RD (2022) Mitochondrial capture and subsequent genetic divergence generates a novel haplogroup: Evidence from ancient and ongoing hybridization in mule and white-tailed deer. Journal of Mammalogy 103(3): 723–736. https://doi.org/10.1093/jmammal/gyab156

Supplementary material 1

Supplementary figure and tables

Authors: Krystal A. Tolley, Devon C. Main, Keith M. Dube, Bettine Jansen van Vuuren, Jessica M. da Silva

Data type: docx

Copyright notice: This dataset is made available under the Open Database License (http://opendatacommons.org/licenses/odbl/1.0/). The Open Database License (ODbL) is a license agreement intended to allow users to freely share, modify, and use this Dataset while maintaining this same freedom for others, provided that the original source and author(s) are credited.

Link: https://doi.org/10.3897/zse.101.151926.suppl1